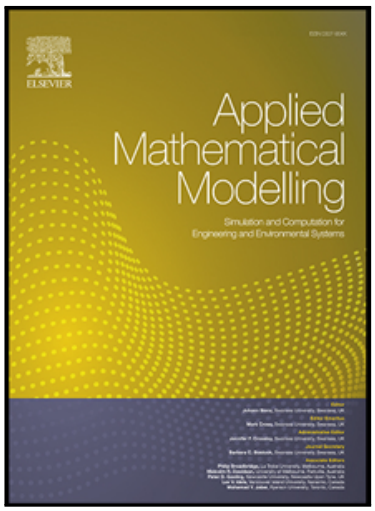

Numerical Solution of Multi-Order Fractional Differential Equations with Multiple Delays via Spectral Collocation Methods

Arman Dabiri, Eric A. Butcher

PII: S0307-904X(17)30742-4
DOI: 10.1016/j.apm.2017.12.012
Reference: APM 12093

To appear in: *Applied Mathematical Modelling*

Received date: 13 May 2017
Revised date: 25 November 2017
Accepted date: 5 December 2017

Please cite this article as: Arman Dabiri, Eric A. Butcher, Numerical Solution of Multi-Order Fractional Differential Equations with Multiple Delays via Spectral Collocation Methods, *Applied Mathematical Modelling* (2017), doi: 10.1016/j.apm.2017.12.012

Highlights

- A framework for solving multi-delay fractional differential equations is proposed.
- Fractional delay differential equiations with irrational delays are disretized.
- The method possesses spectral convergence with efficient computational time.
- The convergence, error estimates, and numerical stability of the method are studied.
- Several illustrative practical examples show the advantages of the method.

Numerical Solution of Multi-Order Fractional Differential Equations with Multiple Delays via Spectral Collocation Methods

Arman Dabiri [*1] and Eric A. Butcher[1]

[1]Department of Aerospace and Mechanical Engineering, University of Arizona

Abstract

This paper discusses a general framework for the numerical solution of multi-order fractional delay differential equations (FDDEs) in noncanonical forms with irrational/ rational multiple delays by the use of a spectral collocation method. In contrast to the current numerical methods for solving fractional differential equations, the proposed framework can solve multi-order FDDEs in a noncanonical form with incommensurate orders. The framework can also solve multi-order FDDEs with irrational multiple delays. Next, the framework is enhanced by the fractional Chebyshev collocation method in which a Chebyshev operation matrix is constructed for the fractional differentiation. Spectral convergence and small computational time are two other advantages of the proposed framework enhanced by the fractional Chebyshev collocation method. In addition, the convergence, error estimates, and numerical stability of the proposed framework for solving FDDEs are studied. The advantages and computational implications of the proposed framework are discussed and verified in several numerical examples for practical engineering problems.

1 Introduction

It is natural to extend the concept of integer derivative orders in differential equations to fractional orders since most natural dynamical phenomena evolve continuously. This expansion has been introduced as a field of mathematics known as fractional calculus. Although fractional calculus has an old history, its applications have been recently found in many areas [1–4]. The list of applications for fractional differential equations (FDEs) has grown rapidly in different fields such as the study of creep or relaxation in visco-elastoplastic materials, diffusion process models, plasma physics, control problems, etc. [5–8]. Besides, delay differential equations (DDEs) occupy a place of central importance in all areas of science with a multitude of practical applications. DDEs are also used in time-delayed systems such as high-speed machining, communication, power systems, and control systems [9]. Including delays in FDEs results in fractional-order delay-differential equations (FDDEs) that are used to model natural phenomena or engineered dynamical systems in a more natural and accurate way [10–12].

The use of efficient and reliable numerical methods for solving differential equations is necessary for a broad range of applications such as engineering problems including model development, control, and simulation. Numerical methods for solving ordinary differential equations include finite difference methods and spectral methods the latter which has exponential converge properties [13, 14].These methods have been also extended to solve FDEs

*armandabiri@email.arizona.edu

including finite-difference method [15–26] and spectral methods [27–33]. Moreover, spectral methods again exhibit superior convergence properties in the sense of having nearly exponential convergence with smaller computation time compared to finite difference methods in solving linear FDEs. The integration of integer-order differential equations has been done locally due to the local property of integer-order derivative operators, but this is no longer applicable for nonlocal fractional-order operators. Thus, the simulation of FDEs is computationally expensive due to the superficial mixture of integer order integral and derivative operators with fractional operators, and hence it is expected to have larger errors in the solution. Several studies have been conducted to address this issue and develop numerically stable methods which indicate the importance of this topic. In contrast to finite difference methods, it is practical to use spectral methods to approximate fractional operators since they are nonlocal. In [28], a comprehensive comparison has been made between the efficiency of using spectral methods to approximate fractional operators and finite difference methods. In recent years, applications of operational matrices have been found in numerical methods [13, 14]. For instance, spectral operational collocation matrices have been used to solve linear FDEs, where the solution is explicitly obtained with spectral convergence and small computational time [28, 29].

The stability analysis of finite difference methods for solving FDEs and FDDEs with a single delay has been studied previously in the literature [34, 35]. Although the stability of linear FDDEs with multiple delays has been studied in the literature [36, 37], there is no study about the stability of numerical methods for solving FDDEs with multiple delays by the use of spectral methods to the best of the authors' knowledge. All previous numerical methods have been mainly developed for solving FDDEs in the canonical form and with a single delay such as using the Grünwald-Letnikov (GL) definition [11, 38], the Adams-Bashforth-Morton method [39, 40], the fractional backward difference method [38], and the Hermite wavelet method [41]. However, all the methods mentioned above are very arduous and time-consuming and exhibit linear convergence. Moreover, the topic of numerical solution for FDEs in noncanonical form with incommensurate orders has not been explored extensively.

In addition, many of the spectral methods mentioned above have been developed without a proper convergence analysis. Comprehensive studies of the convergence analysis of FDEs by spectral methods can be found in a few studies, see [42–45] and references therein. For solving FDDEs by spectral methods, there is no study about the convergence and error estimates, which is one of the aims of this paper. Another critical issue in this topic is the lack of available convenient and reliable numerical packages that can be used by researchers without developing their tools. A few packages have been developed for numerical computation of FDEs [46–49], but all these toolboxes have been mainly developed for control purposes. They are based on approximations of fractional-order differentiator or integrator operators in the Laplace domain [46]. Consequently, there is no sophisticated package in MATLAB for solving FDEs, especially those in noncanonical form with incommensurate orders or multiple delays. Consequently, a freely available package in MATLAB has been developed for solving FDDEs with multi-delays based on the proposed framework for spectral collocation methods. The package including all the examples are available in [50].

The present paper is devoted to proposing a framework for solving multi-order FDDEs with multiple delays based on a spectral collocation method. The proposed framework can be used to solve a system of multi-order FDDEs with commensurate/incommensurate orders and in canonical or noncanonical forms. Multi-order FDDEs with irrational multiple delays can be also solved in this framework. The proposed framework is enhanced with the fractional Chebyshev collocation (FCC) method. This method is an extension of the authors' recent proposed technique that has been implemented for control and stabilization of

fractional periodic time-delay systems, c.f. [51]. The FCC method has spectral convergence and smaller computation time compared to previously proposed methods for solving multi-order FDEs. Next, the convergence and error estimates of the proposed method are studied in Sobolev norms. In addition, the numerical stability of the proposed framework for solving linear FDEs and FDDEs is studied. Several numerical examples with practical applications are presented to confirm the validity and the efficiency of the proposed framework enhanced with the FCC method. Furthermore, the validity and convergence of the proposed FCC framework are compared to the Adams-Bashforth-Moulton method for solving FDEs in the canonical form [15] and the `dde23` solver in MATLAB for solving integer-order DDEs [52].

The rest of the paper is organized as follows. An overview of fractional-order derivative definitions is provided in Section 2. Section 3 is one of the main contributions of the paper where after introducing some discretization operators, the fractional Chebyshev differentiation matrix is derived at Chebyshev-Gauss-Lobatto (CGL) points by using the discrete orthogonality relationship for the Chebyshev polynomials. Next, the discretized state transition matrices are obtained for a system of linear FDEs in canonical and noncanonical forms, and then this concept is extended to find the transition matrix of a system of linear time-varying FDDEs with irrational multiple delays. In Section 4, the numerical stability of the proposed framework for solving linear FDEs and FDDEs is studied. Section 5 is devoted to convergence analysis and error estimates of the proposed method. This section is followed by several illustrative examples in Section 6. Finally, the main results are summarized in Section 7.

2 Preliminaries and Problem Statement

In this section, some basic definitions and notations for fractional calculus are presented.

2.1 Preliminaries

Definition 2.1. Let $f(x)$ be a continuous and integrable function in $[a, x]$. Then the Cauchy formula for repeated integration reduces to a linear Volterra equation of the first kind with kernel $\frac{x^{n-1}}{(n-1)!}$ defined by [53]

$$J^n[f(x)] = \int_a^x \int_a^{\sigma_1} \cdots \int_a^{\sigma_{n-1}} f(\sigma_n)\, \mathrm{d}\sigma_n \cdots \mathrm{d}\sigma_2\, \mathrm{d}\sigma_1 = \frac{1}{(n-1)!} \int_a^x (x-\zeta)^{n-1} f(\zeta)\, \mathrm{d}\zeta, \quad x > a, \tag{1}$$

where $a,\ \zeta \in \mathbb{R}$.

Definition 2.2. The left-sided Riemann-Liouville (RL) fractional integral of order α, $\alpha \in \mathbb{R}^+$, for a function $f(x)$ is defined by a generalization of n in Eq. (1) to a fractional number α as

$${}_a\mathcal{J}_x^{\alpha}[f(x)] = \frac{1}{\Gamma(\alpha)} \int_a^x f(\zeta)\,(x-\zeta)^{\alpha-1}\, d\zeta, \quad x > a, \tag{2}$$

where $\Gamma(.)$ denotes the known Gamma function.

Definition 2.3 ([5])**.** The left-sided RL derivative is defined by pre-multiplying of the fractional-order RL integral operator with the integer-derivative operator, i.e.

$${}_a^{RL}\mathcal{D}_x^{\alpha}[f(x)] = \frac{d^{\lceil \alpha \rceil}}{dx^{\lceil \alpha \rceil}}\, {}_a\mathcal{J}_x^{\lceil \alpha \rceil - \alpha}[f(x)], \quad x > a, \tag{3}$$

where $\lceil . \rceil$ is the ceiling function.

Definition 2.4 ([54]). The left-sided Caputo derivative is defined by pre-multiplying of the integer-derivative operator with the fractional-order RL integral operator, i.e.

$$ {}_a^C\mathcal{D}_x^\alpha[f(x)] =_a \mathcal{J}_x^{\lceil\alpha\rceil-\alpha}\,[\partial_x^{\lceil\alpha\rceil} f(x)], \quad x > a. \tag{4} $$

Property 2.1 (Property 2.1 [53]). *For the power function $x(t) = (t-a)^\beta$, $\beta \in \mathbb{R}$, fractional derivatives in the sense of Caputo with the lower terminal $t_0 = a$ are obtained as*

$$ {}_a^C\mathcal{D}_t^\alpha[(t-a)^\beta] = \begin{cases} \frac{\Gamma(\beta+1)}{\Gamma(\beta+1-\alpha)}(t-a)^{\beta-\alpha}, & \beta \neq 0, \\ 0, & \beta = 0. \end{cases} \tag{5} $$

Definition 2.5 ([5]). The left-sided GL derivative is defined by a finite difference series where the factorial operator replaced by a continuous gamma function as

$$ {}_a^{GL}\mathcal{D}_x^\alpha[f(x)] = \lim_{h\to 0} \frac{1}{h^\alpha} \sum_{k=0}^{k=\frac{x-a}{h}} \frac{\Gamma(\alpha+1)}{k!\,\Gamma(\alpha-k+1)}(-1)^k f(x-kh). \tag{6} $$

2.2 Problem Statement

The current numerical methods are mainly developed for fractional order systems in the canonical form of

$$ {}_a^C\mathcal{D}_t^\alpha[\mathbf{x}(t)] = \mathbf{f}(t, \mathbf{x}, \mathbf{x}(t-\tau)), \quad 0 < \alpha \leq 1, \tag{7} $$

where $\mathbf{x}(t) \in \mathbb{R}^n$, $\mathbf{f}(t, \mathbf{x}, \mathbf{x}(t-\tau)) \in \mathbb{R}^n$, and $\tau \in \mathbb{R}$ is a single delay.

However, in many mathematical modeling, the governing equations are not usually obtained in the form of Eq. (7). Moreover, it is shown that using fractional order dampers with the constitutive equation $F_c(t) = cx^{(\alpha)}(t)$, where c is the fractional damping coefficient and α is the fractional order of the fractional damper, results in more realistic mechanical models' response [55]. As an application of fractional dampers, it has been shown that using fractional viscoelastic models solves several issues in impact models specifically in the impact force-displacement curve [55]. Figure 1 illustrates an impact problem where a rigid body with mass m strikes a flat surface with initial velocity v_0. The surface can be modeled by a fractional K-V model with a fractional damper whose constitutive equation is $F(t) = kx + c\,{}_0^C\mathcal{D}_t^\alpha x(t)$ where k denotes the stiffness. The governing equation of this impact problem is obtained by using the Newton's second law yields the following multi-term FDE:

$$ \ddot{x} + 2\zeta\omega_n\,{}_0^C\mathcal{D}_t^\alpha[x(t)] + \omega_n^2 x = 0, \tag{8} $$

where $\omega_n = \sqrt{k/m}$ is the natural frequency and $\zeta = c/2\sqrt{km}$ is the damping ratio.

Another example is the Beck's column with a non-conservative periodic retarded follower force shown in Fig. 2.2, which can be modeled by a discrete-mass system such as a double inverted pendulum with fractional dampers (see [51, 56]). The load magnitude $\bar{P}$ consists of both constant (P_s) and time periodic components ($P_d \cos(\Omega t)$) acting at an angle proportional by a constant λ to the end of column slope at a previous time $t-\tau$, Ω is the parametric forcing frequency, and τ is a constant delay period equal to the period of the system. The normalized values of the mass and length shown in the figure are assumed to be $m_1 = m_2 = 1\,\text{kg}$, $l_1 = l_2 = 1\,\text{m}$, $c_{f1} = c_{f2} = c_f$, $k_1 = k_2 = k$, and the plane of the double inverted pendulum is assumed to be horizontal such that the equations of motion are not affected by the gravity field. The governing equations of the system can be written as [57]

$$ \begin{bmatrix} 3 & 1 \\ 1 & 1 \end{bmatrix} \begin{bmatrix} \ddot{\theta}_1(t) \\ \ddot{\theta}_2(t) \end{bmatrix} + k \begin{bmatrix} 2 & -1 \\ -1 & 1 \end{bmatrix} \begin{bmatrix} \theta_1(t) \\ \theta_2(t) \end{bmatrix} + \quad c_f \begin{bmatrix} 2 & -1 \\ -1 & 1 \end{bmatrix} \begin{bmatrix} {}_0^C\mathcal{D}_t^\alpha\theta_1(t) \\ {}_0^C\mathcal{D}_t^\alpha\theta_2(t) \end{bmatrix} = p(t, \tau) \tag{9} $$

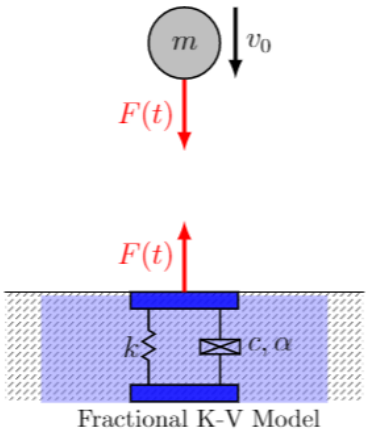

Figure 1: The impact of the mass m colliding with a flat surface modeled by a fractional K-V model with a fractional damper.

where $\mathbf{x}(t) = \left[\theta_1(t), \dot{\theta}_1(t), \theta_2(t), \dot{\theta}_2(t)\right]^T$ denotes the state vector, k is the spring stiffness, c_f is the damping coefficient with fractional order α, and the follower force is in the form of

$$p(t,\tau) = \bar{P}\begin{bmatrix}1 & 0\\ 0 & 1\end{bmatrix}\begin{bmatrix}\theta_1(t)\\ \theta_2(t)\end{bmatrix} - \bar{P}\begin{bmatrix}0 & \lambda\\ 0 & \lambda\end{bmatrix}\begin{bmatrix}\theta_1(t-\tau)\\ \theta_2(t-\tau)\end{bmatrix}. \tag{10}$$

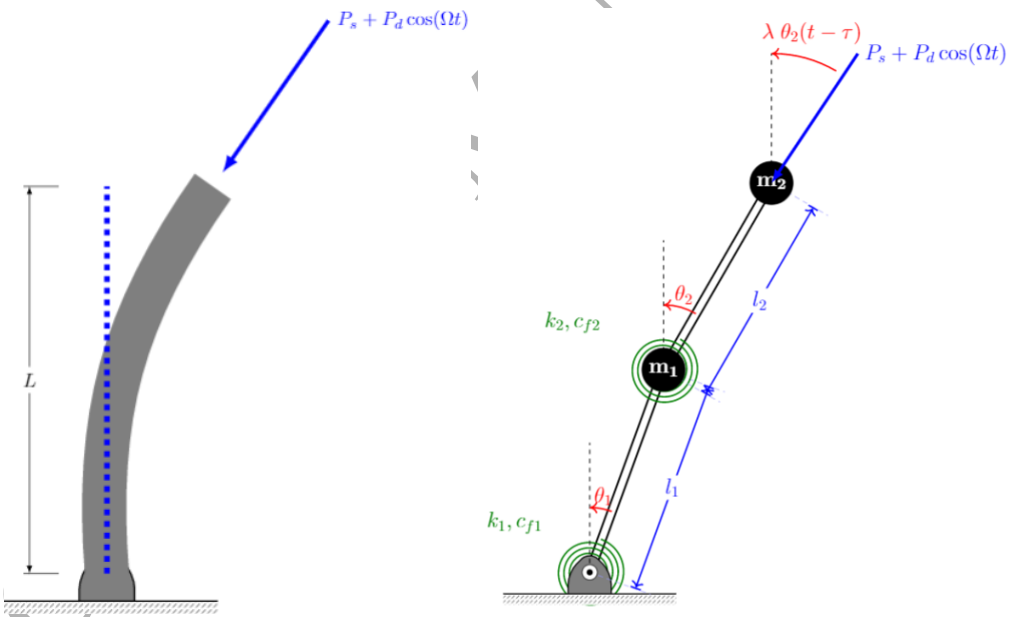

(a) (b)

Figure 2: (a) The Beck's column with a (non-conservative) periodic retarded follower load (b) The discrete-mass model of the Beck's column with the double inverted pendulum with two fractional dampers.

None of Eqs. (8) and (9) represents in the standard canonical form of Eq. (7). Indeed, deriving the governing equation of many mechanical, electrical, and control systems with fractional terms results in linear multi-order FDDEs with multiple delays. Inhere, transforming FDDEs from a noncanonical form to the canonical form is not interested, and it is assumed that a system of multi-order FDDEs with multiple delays $0 < \tau_1 < \tau_2 < \cdots < \tau_s$ is

given as

$$
\begin{aligned}
&{}_0^C\mathcal{D}_t^{(\alpha_1,\cdots,\alpha_n)}[\mathbf{x}(t)] = \\
&\mathbf{f}(t,\mathbf{x}(t),{}_0^C\mathcal{D}_t^{\beta_1}[\mathbf{x}(t)],\cdots,{}_0^C\mathcal{D}_t^{\beta_m}[\mathbf{x}(t)],{}_0^C\mathcal{D}_t^{\nu_1}[\mathbf{x}(t-\tau_1)],\cdots,{}_0^C\mathcal{D}_t^{\nu_s}[\mathbf{x}(t-\tau_s)]) \\
&\text{s.t.} \quad \mathbf{x}(t) = \mathbf{\Phi}(t),\ -\tau_s \le t \le 0,
\end{aligned} \tag{11}
$$

where $\mathbf{x}(t) = [x_1(t),\cdots,x_n(t)]^T \in \mathbb{R}^n$, $\mathbf{\Phi}(t) = [\phi_1(t),\phi_2(t),\cdots,\phi_n(t)]^T$, $\mathbf{f} \in \mathbb{R}^n$, $\alpha_i \in [0,1]$, $i = 1,2,\cdots,n, 0 \le \beta_j,\nu_k < \min\{\alpha_1,\cdots,\alpha_n\}, j = 1,2,\cdots,m, k = 1,2,\cdots,s$, ${}_0^C\mathcal{D}_t^{(\alpha_1,\cdots,\alpha_n)}[\mathbf{x}(t)]$ is defined as

$${}_0^C\mathcal{D}_t^{(\alpha_1,\cdots,\alpha_n)}[\mathbf{x}(t)] := \left[{}_0^C\mathcal{D}_t^{\alpha_1}[x_1(t)],\ {}_0^C\mathcal{D}_t^{\alpha_2}[x_2(t)],\ \cdots,\ {}_0^C\mathcal{D}_t^{\alpha_n}[x_n(t)]\right]^T, \tag{12}$$

and ${}_0^C\mathcal{D}_t^{\alpha}[\mathbf{x}(t)]$ is

$${}_0^C\mathcal{D}_t^{\alpha}[\mathbf{x}(t)] := \left[{}_0^C\mathcal{D}_t^{\alpha}[x_1(t)],\ {}_0^C\mathcal{D}_t^{\alpha}[x_2(t)],\ \cdots,\ {}_0^C\mathcal{D}_t^{\alpha}[x_n(t)]\right]^T, \tag{13}$$

It is worthy to mention that $\boldsymbol{\alpha}$, $\boldsymbol{\beta}$, and $\boldsymbol{\nu}$ can be irrational or incommensurate orders.

There are three standard methods to solve FDDEs in Eq. (41): (1) using the conventional numerical integration methods for solving ordinary differential equations when the fractional differentiation operator in Eq. (11) can be approximated by the integer-order differentiation operator, (2) using the standard numerical methods for integrating FDEs in canonical form if FDDEs in Eq. (41) can be transformed to the form of Eq. (7), (3) discretizing the FDDEs in Eq. (41) by the discretization of the fractional differentiation operator. However, in the first method, approximating fractional differentiation operators as integer-order differentiation operators is not possible always and straightforward. In the second method, transforming and initializing FDDEs in a noncanonical form to FDDEs with a canonical form is still an open problem [58–60]. Although the third method does not have the limitations of the previously methods mentioned above, it has been only developed for FDDEs with a single delay [38,40,41].

In the next section, a framework for spectral collocation methods is introduced to solve multi-term FDDEs with multiple delays, which do not need to be in the canonical form or with commensurate orders.

3 Discretization Framework for Spectral Collocation Method

In this section, the framework of using spectral collocation method for discretization of systems of commensurate FDEs and FDDEs with multiple delays is described. For this purpose, first, a few discretization operators are proposed. The fractional differentiation matrix in the sense of Caputo is derived by using the CGL points. Next, steps for discretizing the solution of the system at some collocation points are detailed. In addition, a state transition matrix is defined for the discretized solution of linear systems with the initial condition $x_0 = x(0)$ in $[0,\tau]$. Then, the theory is extended to solve a system of FDDEs with irrational multiple delays.

Definition 3.1. The discretized vector and modified discretized vector of the function $p(t)$ at the collocation points $\mathbf{t} = [t_0,t_1,\cdots,t_{N-1}]^T$ are defined by

$$\mathbf{p}_{d_\mathbf{t}} := \left[p(t_0),\ p(t_1),\ \cdots,p(t_{N-1})\right]^T, \tag{14a}$$

$$\overline{\mathbf{p}}_{d_\mathbf{t}} := \left[0,\ p(t_1),\ \cdots,p(t_{N-1})\right]^T, \tag{14b}$$

(14c)

respectively. In the case that $p(t)$ is a constant p_0, its discretized vector is

$$\mathbf{p}_{d_t} := p_0\mathbf{1}, \tag{15a}$$
$$\overline{\mathbf{p}}_{d_t} := p_0\overline{\mathbf{1}}, \tag{15b}$$

where $\mathbf{1}$ is $N \times 1$ column vector of all ones and $\overline{\mathbf{1}}$ is a modified $\mathbf{1}$ whose first element is set to zero.

Definition 3.2. The discretized vector and modified discretized vector of an $n \times 1$ column vector of $\mathbf{u} := [u_1, u_2, \cdots, u_n]^T$ at the collocation points $\mathbf{t} = [t_0, t_1, \cdots, t_{N-1}]^T$ are defined by

$$\mathbf{u}_{d_t} := [\mathbf{u}_{1,d}^T, \mathbf{u}_{2,d}^T, \cdots, \mathbf{u}_{n,d}^T]^T, \tag{16a}$$
$$\overline{\mathbf{u}}_{d_t} := [\overline{\mathbf{u}}_{1,d}^T, \overline{\mathbf{u}}_{2,d}^T, \cdots, \overline{\mathbf{u}}_{n,d}^T]^T, \tag{16b}$$

respectively.

Definition 3.3. The discretized matrix of the $n \times m$ matrix function $P(t)$ with elements $p_{ij}(t)$, $i = 1, 2, \cdots, n$, $j = 1, 2, \cdots, m$, $(m, n > 1)$, at the collocation points $\mathbf{t} = [t_0, t_1, \cdots, t_{N-1}]^T$ is given by

$$P_{d_t} := \begin{bmatrix} \text{diag}\left(\mathbf{p}_{11,d_t}\right) & \cdots & \text{diag}\left(\mathbf{p}_{1m,d_t}\right) \\ \vdots & \ddots & \vdots \\ \text{diag}\left(\mathbf{p}_{n1,d_t}\right) & \cdots & \text{diag}\left(\mathbf{p}_{nm,d_t}\right) \end{bmatrix}, \tag{17}$$

where $\mathbf{p}_{ij,d_t}$, $i = 1, 2, \cdots, n$, $j = 1, 2, \cdots, m$, are the discretized vectors of $p_{ij}(t)$ given by Definition 3.1 and $\text{diag}(v)$ returns a square diagonal matrix with the elements of the vector v on the main diagonal.

Definition 3.4. The modified discretized matrix of the $n \times m$ matrix function $P(t)$ at the collocation points $\mathbf{t} = [t_0, t_1, \cdots, t_{N-1}]^T$ is given by

$$\overline{P}_{d_t} := (I_N \otimes \overline{I}_n) P_{d_t}, \tag{18}$$

where I_n and $\overline{I}_n$ are defined as the $n \times n$ identity matrix and $n \times n$ identity matrix that its first element replaced by zero, respectively, and $\otimes$ is the Kronecker operator.

Definition 3.5. The discretization operators $\{\underline{\mathbf{u}}\}_{d_t}$ are $\{\overline{\mathbf{u}}\}_{d_t}$ for an $n \times 1$ constant vector $\mathbf{u} = [u_1, u_2, \cdots, u_n]^T$ at the collocation points $\mathbf{t} = [t_0, t_1, \cdots, t_{N-1}]^T$ are defined as

$$\{\overline{\mathbf{u}}\}_{d_t} := u \otimes \overline{\mathbf{0}}, \tag{19a}$$
$$\{\underline{\mathbf{u}}\}_{d_t} := u \otimes \underline{\mathbf{0}}, \tag{19b}$$

where $\overline{\mathbf{0}}$ and $\underline{\mathbf{0}}$ are $N \times 1$ column vectors of all zeros expect their first and last element are modified to one, respectively.

3.1 Fractional Chebyshev Differentiation Matrix

Definition 3.6 ([28]). The discretized matrix of ${}_{t_0}^{C}\mathcal{D}_t^{\alpha}[\cdot]$ at the collocation points $\mathbf{t} = [t_0, t_1, \cdots, t_{N-1}]$ is named fractional differentiation matrix and denoted by $\mathrm{D}_{d_t}^{\alpha}$. It is a linear map that maps the discretized function $\mathbf{x}_{d_t}$ onto the discretized value of ${}_{t_0}^{C}\mathcal{D}_t^{\alpha}[x(t)]$ at those points as

$$\mathrm{D}_{d_t}^{\alpha}\mathbf{x}_{d_t} = \left[\left[{}_{t_0}^{C}\mathcal{D}_t^{\alpha}[x(t)]\right]_{t=t_0} \quad \left[\mathcal{D}_t^{\alpha}[x(t)]\right]_{t=t_1} \quad \cdots \quad \left[{}_{t_0}^{C}\mathcal{D}_t^{\alpha}[x(t)]\right]_{t=t_{N-2}} \quad \left[{}_{t_0}^{C}\mathcal{D}_t^{\alpha}[x(t)]\right]_{t=t_{N-1}} \right]^T. \tag{20}$$

A fractional differentiation matrix can be constructed by the interpolation of a mth-degree polynomial on m points of the grid points [28]. Furthermore, a finite difference fractional differentiation matrix is obtained by interpolation of a local mth-degree polynomial on m local points of an equispaced grid. This local-interpolation for low degree polynomial results in a maximum accuracy $O(h^m)$ for differentiating a function.

Theorem 3.1 ([28]). *The fractional finite difference differentiation matrix in the sense of Caputo at uniform collocation points* $\mathbf{t} = [t_0 = a, t_1, \cdots, t_{N-1} = b]$ *with the fixed step* $h = \frac{b-a}{N-1}$ *is*

$$\mathrm{D}^{\alpha}_{d_{\mathbf{t}}} := \frac{1}{h^{\alpha}\Gamma(2-\alpha)} \begin{bmatrix} 0 & 0 & 0 & 0 & \cdots & 0 & 0 \\ a_1 & 1 & 0 & \ddots & \ddots & 0 & 0 \\ a_2 & b_1 & 1 & 0 & \ddots & \ddots & 0 \\ a_3 & b_2 & b_1 & 1 & 0 & \ddots & 0 \\ \vdots & \ddots & \ddots & \ddots & 1 & 0 & 0 \\ a_{N-2} & b_{N-3} & \ddots & b_2 & b_1 & 1 & 0 \\ a_{N-1} & b_{N-2} & b_{N-3} & \cdots & b_2 & b_1 & 1 \end{bmatrix} \tag{21}$$

where $a_k = (k-1)^{1-\alpha} - k^{1-\alpha}$ *and* $b_k = (k-1)^{1-\alpha} - 2k^{1-\alpha} + (k+1)^{1-\alpha}$.

Increasing the degree of the polynomial does not decrease the interpolation error because of the unbounded growth in round-off errors. One practical technique to overcome this issue is the use of inequispaced collocation points which is the basic concept of spectral methods. The main idea of spectral methods is the use of a global Nth-degree polynomial that employs all the N collocation points inside the domain and achieves the maximum accuracy. It has been shown that interpolation at the CGL points bounds the interpolation error and obtains the minimum error out of all sets of collocation points [14]. The CGL points can be interpreted as the projections of equispaced points on the upper half of the unit circle, and hence they are non-equispaced points and distributed more densely towards the edges of the interval. The CGL points are given by extreme points of the first kind Chebyshev polynomials $T_n(\xi)$, i.e. $\xi_j = \cos(j\pi/N-1)$, $j = 0, 1, \cdots, N-1$, in $[-1, 1]$. Therefore, the Chebyshev polynomials are ideal to be used in spectral methods.

Let $\Lambda = [-1, 1]$ and $\xi \in \Lambda$. Then, the nth-degree Chebyshev polynomial of the first kind $T_n(\xi)$ is defined by the formula

$$T_n(\xi) = \cos(n \arccos(\xi)), \tag{22}$$

and its recurrence relation is

$$T_n(\xi) = 2\xi T_{n-1}(\xi) - T_{n-2}(\xi), \quad n = 2, 3, \cdots, \tag{23}$$

with $T_0(\xi) = 1$ and $T_1(\xi) = \xi$. Moreover, we have

$$T_n(x) = \frac{n}{2} \sum_{k=0}^{\lfloor \frac{n}{2} \rfloor} (-1)^k \frac{(n-k-1)!}{k!(n-2k)!} \, 2^{n-2k} \, x^{n-2k}, \qquad n \in \mathbb{N}, \tag{24}$$

We are, however, interested in a more general interval $\Omega = [a, b]$ instead of $\Lambda = [-1, 1]$ in most of engineering problems. Thus, the shifted Chebyshev polynomials denoted by $T^{\star}_N(\cdot)$ are more interested. The shifted Chebyshev polynomials are defined by changing of the variable ξ in the Chebyshev polynomials as $\xi = \frac{2}{h}(t-a) - 1$ where $h = b - a$ .Thus, $T^{\star}_N(t)$ can be obtained as

$$T^{\star}_N(t) = T_N(\frac{2}{h}(t-a) - 1), \quad t \in \Lambda^{\star}. \tag{25}$$

The weight associate with the $L^2_{w^{\star}}(\Omega)$ is $w^{\star}(t) = w(\frac{2}{h}(t-a) - 1)$.

Proposition 3.1. *Let $\Lambda^\star = [0,1]$ and $t \in \Lambda^\star$. The fractional Chebyshev differentiation matrix in the sense of Caputo at the CGL points $\mathbf{t} = [t_0 = 0, t_1, \cdots, t_{N-1} = 1]$ is defined by*

$$\mathrm{D}^{\alpha}_{d_{\mathbf{t}}} = \begin{bmatrix} {}_0^C\mathcal{D}_t^\alpha[T_0^\star(t)]]_{t_0} & {}_0^C\mathcal{D}_t^\alpha[T_1^\star(t)]]_{t_0} & \cdots & {}_0^C\mathcal{D}_t^\alpha[T_{N-1}^\star(t)]]_{t_0} \\ {}_0^C\mathcal{D}_t^\alpha[T_0^\star(t)]]_{t_1} & {}_0^C\mathcal{D}_t^\alpha[T_1^\star(t)]]_{t_1} & \cdots & {}_0^C\mathcal{D}_t^\alpha[T_{N-1}^\star(t)]]_{t_1} \\ \vdots & \vdots & \ddots & \vdots \\ {}_0^C\mathcal{D}_t^\alpha[T_0^\star(t)]]_{t_{N-1}} & {}_0^C\mathcal{D}_t^\alpha[T_1^\star(t)]]_{t_{N-1}} & \cdots & {}_0^C\mathcal{D}_t^\alpha[T_{N-1}^\star(t)]]_{t_{N-1}} \end{bmatrix} H. \tag{26}$$

where

$$H = \frac{1}{N-1}\begin{bmatrix} \frac{1}{2} & 1 & \cdots & 1 & \frac{1}{2} \\ (-1)^1 & 2T_1^\star(t_1) & \cdots & 2T_1^\star(t_{N-1}) & 1 \\ \vdots & \vdots & \ddots & \vdots & \vdots \\ (-1)^{N-2} & 2T_{N-1}^\star(t_1) & \cdots & 2T_{N-1}^\star(t_{N-1}) & 1 \\ \frac{(-1)^{N-1}}{2} & T_N^\star(t_1) & \cdots & T_N^\star(t_{N-1}) & \frac{1}{2} \end{bmatrix}. \tag{27}$$

Proof. Let function $x(t)$ belong to the $L^2_{w^\star}(\Lambda^\star)$ space with a weight $w^\star(t) = 1/\sqrt{1-(2t-1)^2}$. The function $x(t)$ can be approximated by the use of the shifted Chebyshev polynomials as

$$x(t) \approx \sum_{k=0}^{N-1} \hat{x}_k T_k^\star(t), \tag{28}$$

where $\hat{x}_k \in \mathbb{R}$, $k = 0, 1, \cdots, N-1$, are called shifted Chebyshev coefficients and can be obtained by the discrete orthogonality relationship for the shifted Chebyshev polynomials as

$$\sum_{k=0}^{N-1} \frac{1}{c_k} T_i^\star(t_k) T_j^\star(t_k) = \frac{c_i}{2}(N-1)\delta_{ij}, \quad c_i = \begin{cases} 2, & i = 0 \text{ or } N-1, \\ 1, & i \neq 0 \text{ or } N-1, \end{cases} \tag{29}$$

in which δ_{ij} denotes the Kronecker delta. Using Eq. (29) and Eq. (28) yields

$$\hat{x}_k = \frac{2}{(N-1)c_k} \sum_{i=0}^{N-1} \frac{1}{c_i} T_k^\star(t_i) x(t_i), \quad k = 0, 1, \ldots, N-1. \tag{30}$$

The shifted Chebyshev coefficients can be obtained by the matrix H defined in Eq. (27). Let $\hat{\mathbf{x}}$ and $\mathbf{x}_{d_{\mathbf{t}}}$ be the shifted Chebyshev coefficient vector and discretized values of $x(t)$ at the CGL points, respectively, then $\hat{\mathbf{x}} = H\mathbf{x}_{d_{\mathbf{t}}}$. Thus, the approximation in Eq. (28) can be rewritten in vector form by substituting Eq. (27) into Eq. (28) as

$$x(t) \approx \mathbf{T}^T(t) H \mathbf{x}_{d_{\mathbf{t}}}, \tag{31}$$

where $\mathbf{T}(t) = [T_0^\star(t), \cdots, T_N^\star(t)]^T$.

□

Corollary 3.1 ([28]). *Let $\mathrm{D}^{\alpha}_{d_{\mathbf{t}}}$ and $\mathrm{D}^{\alpha}_{d_{\mathbf{z}}}$ denote the Chebyshev fractional differentiation matrix for $\mathbf{t}$ in $[0,1]$ and $\mathbf{z}$ in $[a,b]$, respectively. Then*

$$\mathrm{D}^{\alpha}_{d_{\mathbf{z}}} = \frac{1}{(b-a)^\alpha} \mathrm{D}^{\alpha}_{d_{\mathbf{t}}} \tag{32}$$

Recently, different methods such as power methods [28] and recurrence methods [29] have been proposed to obtain the fractional Chebyshev differentiation matrix in Definition 3.6. The main advantage of these methods is that they are not limited to the size or the number of the collocation points.

3.2 Multi-Order Fractional Differential Equations

Consider the following linear multi-order FDEs in the noncanonical representation

$$ {}_0^C\mathcal{D}_t^{(\alpha_1,\cdots,\alpha_n)}[\mathbf{x}(t)] = A(t)\,\mathbf{x}(t) + \sum_{j=1}^{m} G_j(t)\,{}_0^C\mathcal{D}_t^{\beta_j}[\mathbf{x}(t)] + \mathbf{b}(t), \quad t_0 \le t \le \tau, \tag{33} $$

subject to the initial conditions $\mathbf{x}_0 = [x_{01},\cdots,x_{0n}]^T$ where $\mathbf{x}(t) = [x_1(t),\cdots,x_n(t)]^T$, $x_i(t) \in \mathbb{R}$, $i = 1,2,\cdots,n$, $A(t) \in \mathbb{R}^{n\times n}$, $G_j(t) \in \mathbb{R}^{n\times n}$, $j = 1,2,\cdots,r$, $\mathbf{b}(t) \in \mathbb{R}^n$, $\alpha_i \in [0,1]$, $i = 1,2,\cdots,n$, $0 \le \beta_j < \min\{\alpha_1,\cdots,\alpha_n\}$, $j = 1,2,\cdots,m$, and ${}_0^C\mathcal{D}_t^{(\alpha_1,\cdots,\alpha_n)}[\mathbf{x}(t)]$ is defined in Eq. (12).

Proposition 3.2. *The discretized solution of Eq. (33) is given by*

$$ \mathbf{x}_{d_t} = T_{d_t}\left(\overline{\mathbf{b}}_{d_t} + \{\overline{\mathbf{x}}_0\}_{d_t}\right), \quad t_0 \le t \le \tau, \tag{34} $$

where

$$ {}_aT_{d_t} = \left(\overline{\mathbb{D}}_{d_t}^{(\alpha_1,\cdots,\alpha_n)} - \overline{A}_{d_t} - \sum_{j=1}^{r}\overline{G}_{j\,d_t}\mathbb{D}_{d_t}^{(\beta_j)} + I_n\otimes J\right)^{-1}, \quad t_0 \le t \le \tau, \tag{35} $$

such that $\det\left({}_aT_{d_t}^{-1}\right) \neq 0$, *where* $\overline{A}_{d_t}$ *and* $\overline{G}_{j\,d_t}$ *are the* $nN\times nN$ *and* $nN\times nN$ *modified discretized matrices associated with* $A(t)$ *and* $G_j(t)$ *obtained by Definition 3.4,* $\overline{\mathbf{b}}_{d_t}$ *is the* $1\times nN$ *discretized vector associated with* $\mathbf{b}(t)$ *obtained by Definition 3.2,* $\{\overline{\mathbf{x}}_0\}_{d_t}$ *for* x_0 *is given by Definition 3.5,* J *is* $N\times N$ *zero matrix with its first row replaced by* $[1,0,0,\cdots,0,0]$, *and*

$$ \overline{\mathbb{D}}_{d_t}^{(\alpha_1,\cdots,\alpha_n)} = (I_n\otimes\bar{I}_N)\,\mathrm{blkdiag}\left\{\mathrm{D}_{d_t}^{\alpha_1},\ \mathrm{D}_{d_t}^{\alpha_2},\ \cdots,\ \mathrm{D}_{d_t}^{\alpha_n}\right\}, \tag{36a} $$

$$ \mathbb{D}_{d_t}^{(\beta_j)} = I_n\otimes\mathrm{blkdiag}\left\{\mathrm{D}_{d_t}^{\beta_j},\ \mathrm{D}_{d_t}^{\beta_j},\ \cdots,\ \mathrm{D}_{d_t}^{\beta_j}\right\}, \tag{36b} $$

in which $\bar{I}_N$ *is defined in Eq. (18) and* $\mathrm{blkdiag}\,(A_1,A_2,...,A_n)$ *constructs a block diagonal matrix from the input matrices* A_i.

Proof. Substituting the state transition matrix (35) into Eq. (34) and rearranging it yields

$$ \left(\overline{\mathbb{D}}_{d_t}^{(\alpha_1,\cdots,\alpha_n)} + I_n\otimes J\right)\mathbf{x}_{d_t} = \overline{A}_{d_t}\mathbf{x}_{d_t} + \sum_{j=1}^{r}\overline{G}_{j\,d_t}\mathbb{D}_{d_t}^{(\beta_j)}\mathbf{x}_{d_t} + \overline{\mathbf{b}}_{d_t} + \{\overline{\mathbf{x}}_0\}_{d_t}. \tag{37} $$

Since all the elements of the iNth rows, $i = 1,2,\cdots,n$, of all the discretized matrices in Eq. (37) (i.e. $\overline{\mathbb{D}}_{d_t}^{(\boldsymbol{\alpha})}$, $\overline{A}_{d_t}$, $\overline{G}_{j\,d_t}\mathbb{D}_{d_t}^{(\beta_j)}$, and $\overline{\mathbf{b}}_{d_t}$) are zero except that of the $\{\overline{\mathbf{x}}_0\}_{d_t}$ which are equal to x_{0i}, $i = 1,2,\cdots,n$, we have $\left[\mathbf{x}_{i\,d_t}\right]_1 = x_i(t_0)$, $i = 1,2,\cdots,n$, where $\left[\mathbf{x}_{i\,d_t}\right]_1$ is the first element of the vector $\mathbf{x}_{i\,d_t}$ that is the discretized vector of $x_i(t)$. In addition, $\overline{\mathbb{D}}_{d_t}^{(\boldsymbol{\alpha})}\mathbf{x}_{d_t}$ is equal to discretized values of ${}_0^C\mathcal{D}_t^{(\boldsymbol{\alpha})}[\mathbf{x}(t)]$ at collocation points $\mathbf{t}$ according to Definition 3.6. Therefore, Eq. (37) is a discretized form of Eq. (34) in $[0,\tau]$. Since the right hand side of Eq. (35) is invertible, there exists a unique solution for the discretized form of Eq. (34). □

Consider the following a system of nonlinear FDEs

$$ {}_0^C\mathcal{D}_t^{(\alpha_1,\cdots,\alpha_n)}[\mathbf{x}(t)] = \mathbf{f}(t,\mathbf{x}(t),{}_0^C\mathcal{D}_t^{\beta_1}[\mathbf{x}(t)],\cdots,{}_0^C\mathcal{D}_t^{\beta_m}[\mathbf{x}(t)]) \tag{38} $$

subject to the initial conditions $\mathbf{x}_0 = [x_{01},\cdots,x_{0n}]^T$ where $\mathbf{f}(\cdot) \in \mathbb{R}^n$, $\alpha_i \in [0,1]$, $i = 1,2,\cdots,n$, $0 \le \beta_j < \min\{\alpha_1,\cdots,\alpha_n\}$, $j = 1,2,\cdots,m$, and $\mathbf{x}(t)$, and ${}_0^C\mathcal{D}_t^{(\alpha_1,\cdots,\alpha_n)}[\mathbf{x}(t)]$ is

defined in Eq. (12). The system of the nonlinear multi-order FDEs in Eq. (38) can be discretized at collocation points $\mathbf{t} = [t_0 = 0, t_1, \cdots, t_{N-1}, t_N = T]$ by approximating the Caputo derivative operators with the fractional differentiation matrices.

Let $\mathbf{x}_{i d_{\mathbf{t}}}^T$, $i = 1, 2, \cdots, n$, denote discretized $x_i(t)$ at collocation points $\mathbf{t}$ such that $\mathbf{x}_{d_{\mathbf{t}}} = [\mathbf{x}_{1 d_{\mathbf{t}}}^T, \cdots, \mathbf{x}_{n d_{\mathbf{t}}}^T]^T$. The discretized solution of the system of the nonlinear multi-order FDEs in Eq. (38) in $t \in [0, T]$ is obtained by solving the following system of nonlinear equations

$$\overline{\mathbb{D}}_{d_{\mathbf{t}}}^{(\alpha_1, \cdots, \alpha_n)} [\mathbf{x}(t)] = \bar{\mathbf{f}}_{d_{\mathbf{t}}} (\mathbf{t}, \mathbf{x}_{d_{\mathbf{t}}}, \overline{\mathbb{D}}_{d_{\mathbf{t}}}^{(\beta_1)} \mathbf{x}_{d_{\mathbf{t}}}, \cdots, \overline{\mathbb{D}}_{d_{\mathbf{t}}}^{(\beta_m)} \mathbf{x}_{d_{\mathbf{t}}}) \tag{39}$$

subject to

$$[\mathbf{x}_{k d_{\mathbf{t}}}]_1 = x_{0k}, \quad k = 0, 1, \cdots, n, \tag{40}$$

where $\bar{\mathbf{f}}_{d_{\mathbf{t}}}$ is the discretized matrix of $\mathbf{f}(t, \mathbf{x}(t), {}_0^C\mathcal{D}_t^{(\beta)}[\mathbf{x}(t)])$ obtained by Definition 3.2. The discretized FDE in Eq. (39) together with the initial conditions in Eq. (40) generate $(n-1) \times N$ nonlinear equations which can be solved using Newton's iteration method to obtain $\mathbf{x}_{d_{\mathbf{t}}}$.

3.3 Multi-Order Fractional Delay-Differential Equations with Multiple Delays

Consider a system of linear multi-order FDDEs with multiple delays

$${}_0^C\mathcal{D}_t^{(\alpha_1, \cdots, \alpha_n)} [\mathbf{x}(t)] = A(t)\, \mathbf{x}(t) + \sum_{j=1}^{m} G_j(t)\, {}_0^C\mathcal{D}_t^{\beta_j} [\mathbf{x}(t)] + \sum_{k=1}^{s} F_k(t)\, {}_0^C\mathcal{D}_t^{\nu_k} [\mathbf{x}(t - \tau_i)] \tag{41}$$

subject to the initial function $\boldsymbol{\phi}(t) = [\phi_1(t), \cdots, \phi_n(t)]^T$, $-\tau_s \le t \le 0$, where $\mathbf{x}(t) = [x_1(t), x_2(t), \cdots, x_n(t)]^T$, $x_i(t) \in \mathbb{R}$, $i = 1, 2, \cdots, n$, $A(t), G_j(t), F_i(t) \in \mathbb{R}^{n \times n}$, $i = 1, 2, \cdots, n$, $j = 1, 2, \cdots, m$, $\alpha_i \in [0, 1]$, $i = 1, 2, \cdots, n$, $0 \le \beta_j, \nu_k < \min\{\alpha_1, \cdots, \alpha_n\}$, $j = 1, 2, \cdots, m$, $k = 1, 2, \cdots, s$, and $0 < \tau_1 < \tau_2 < \cdots < \tau_s$.

Proposition 3.3. *The solution of FDDE (41) in $[0, p\tau_1]$, $p \in \mathbb{N}$, is given by the following equation*

$$\mathbf{x}_{d_{\mathbf{t}_i}} = {}_0T_{d_{\mathbf{t}_i}} \left(\sum_{k=1}^{s} \overline{F}_{k, d_{\mathbf{t}_i}}\, \overline{\mathbb{D}}_{d_{\mathbf{t}_i}}^{(\zeta_k)} \mathbf{x}_{d_{\mathbf{z}_{i,k}}} + \{\underline{\boldsymbol{\phi}}_0\}_{d_{\mathbf{t}}} \right), \quad i = 1, 2, \cdots, p, \tag{42}$$

where $\mathbf{t}_i$ and $\mathbf{z}_{i,k}$ include the N number of discretized points in $[0, i\tau_1]$ and $[-\tau_k, -\tau_k + i\tau_1]$, $i = 1, 2, \cdots, p$, respectively, $\overline{F}_{k, d_{\mathbf{t}_i}}$ are the discretized matrix of $F_k(t)$, $k = 1, 2, \cdots, s$, $\{\underline{\boldsymbol{\phi}}_0\}_{d_{\mathbf{t}}}$ is obtained by Definition 3.5 for $\boldsymbol{\phi}(0)$, and

$${}_0T_{d_{\mathbf{t}_i}} = \left(\overline{\mathbb{D}}_{d_{\mathbf{t}_i}}^{(\alpha_1, \cdots, \alpha_n)} - \overline{A}_{d_{\mathbf{t}_i}} - \sum_{j=1}^{m} \overline{G}_{j\, d_{\mathbf{t}_i}}\, \overline{\mathbb{D}}_{d_{\mathbf{t}_i}}^{(\beta_j)} + I_n \otimes J \right)^{-1} \tag{43}$$

such that $\det\left({}_0T_{d_{\mathbf{t}_i}}^{-1}\right) \neq 0$.

Proof. Begin with obtaining the discretized solution $\mathbf{x}_{d_{\mathbf{t}_1}}$ in $[0, \tau_1]$. The steps are similar to the ones in the proof of Proposition 3.2 where the continuity of the solution at $t = 0$ (i.e. $\boldsymbol{\phi}(0)$) is guaranteed by using the discretization operators in this section. The next solution must be obtained in $[0, 2\tau_1]$ because the lower terminal of the fractional derivative operator is fixed at $t = 0$, i.e. more details about this issue is given in [61]. Therefore, the delayed terms require new mesh grids $\mathbf{z}_{2,k}$, $k = 1, 2, \cdots, s$, in $[-\tau_i, -\tau_i + 2\tau_1]$ (see [61]). In addition, if any $\mathbf{z}_{1,k}$,

$k = 1, 2, \cdots, s$, includes the solution points from $\mathbf{x}_{d_{\mathbf{t}_1}}$, then the points have to be interpolated by an interpolation technique such as the piecewise cubic Hermite interpolating polynomial (PCHIP) since the points $\mathbf{x}_{d_{\mathbf{t}_1}}$ are at inequispaced points. Since $\det\left({}_0T^{-1}_{d_{\mathbf{t}_i}}\right)$ is invertible, there is a unique solution for $\mathbf{x}_{d_{\mathbf{t}_2}}$. These steps can be repeated to obtain the discretized solution $\mathbf{x}_{d_{\mathbf{t}_n}}$ in $[0, n\tau_1]$.

□

Proposition 3.4. *Let FDDE (41) be written as linear DDEs whose coefficient matrices are periodic, its delays be proportional such that $\tau_k = k\tau_0$, $k = 1, \cdots, s$, and τ_0 be a multiple of the principal period T. That is*

$$\dot{\mathbf{x}}(t) = A(t)\,\mathbf{x}(t) + \sum_{i=1}^{s} F_i(t)\,\mathbf{x}(t - i\tau_0), \tag{44}$$

where $A(t+T) = A(t)$ and $F_i(t+T) = F_i(t)$, $i = 1, \cdots, s$. In addition, let $\mathbf{y}_k = \left[\mathbf{x}_{d_{\mathbf{t}_{k,1}}}, \cdots, \mathbf{x}_{d_{\mathbf{t}_{k,s}}}\right]^T$, $k \in \mathbb{N}$, and $\mathbf{w}_0 = \left[\mathbf{x}_{d_{\mathbf{z}_1}}, \cdots, \mathbf{x}_{d_{\mathbf{z}_s}}\right]^T$ where $\mathbf{t}_{k,i}$ and $\mathbf{z}_i$ denote the discretized points in $[(i-1+(k-1)s)\tau_0, (i+(k-1)s)\tau_0]$, and $[-i\tau_0, -(i-1)\tau_0]$, $i = 1, 2, \cdots, s$, respectively. Then, the solution $\mathbf{y}_k$ in $[(k-1)s\tau_0, ks\tau_0]$ is obtained by a monodromy matrix $\mathcal{M}$ such that

$$\mathbf{y}_k = \mathcal{M}^k \mathbf{w}_0, \tag{45}$$

where

$$\mathcal{M} = \left[M_1^T, M_2^T, \cdots, M_s^T\right]^T, \tag{46a}$$

$$M_1 = \left(\overline{\mathbb{D}}^{(\mathbf{1})}_{d_{\mathbf{t}_1}} - \overline{A}_{d_{\mathbf{t}_1}} + I_n \otimes J\right)^{-1} \left[\overline{F}_{1,d_{\mathbf{t}_1}} \;\; \cdots \;\; \overline{F}_{s,d_{\mathbf{t}_1}}\right], \tag{46b}$$

$$M_i = \left(\overline{\mathbb{D}}^{(\mathbf{1})}_{d_{\mathbf{t}_i}} - \overline{A}_{d_{\mathbf{t}_i}} + I_n \otimes J\right)^{-1} \left[\overline{F}_{1,d_{\mathbf{t}_i}} \;\; \cdots \;\; \overline{F}_{s,d_{\mathbf{t}_i}}\right] \left[M_1^T \;\; \cdots \;\; M_{i-1}^T \;\; \mathcal{I}_i^T\right]^T, \tag{46c}$$

$\mathcal{I}_i = \mathcal{J}_{s+1-i} \otimes I_N$, and $\mathcal{J}_n$ is a $n \times sN$ matrix with ones on the main diagonal and zeros elsewhere.

Proof. Similar steps to the ones in the proof of Proposition 3.3 is followed to find the solution $\mathbf{y}_1$ in $[0, s\tau_0]$ yielding $\mathbf{y}_1 = \mathcal{M}\mathbf{w}_0$. Since all the principal period of the coefficient matrices are factor of τ_0 and the differentiation matrix $\mathbb{D}^{(\mathbf{1})}_{d_{\mathbf{t}_i}}$ are equal (as they are dependent on the lower terminal), $\mathcal{M}$ is unique map and the solution $\mathbf{y}_2$ in $[s\tau_0, (s+1)\tau_0]$ can be obtained as $\mathbf{y}_2 = \mathcal{M}\mathbf{y}_1$. Consequently, we have $\mathbf{y}_k = \mathcal{M}\mathbf{y}_{k-1}$, $\mathbf{y}_0 = \mathbf{w}_0$, and this completes the proof.

□

The discretized solution of the nonlinear FDDEs in Eq. (11) can be obtained by solving the following system of nonlinear equations

$$\overline{\mathbb{D}}^{(\alpha_1,\cdots,\alpha_n)}_{d_{\mathbf{t}_i}} \mathbf{x}_{d_{\mathbf{t}_i}} = \overline{\mathbf{f}}_{d_{\mathbf{t}_i}}(\mathbf{t}, \mathbf{x}_{d_{\mathbf{t}_i}}, \overline{\mathbb{D}}^{(\beta_1)}_{d_{\mathbf{t}_i}} \mathbf{x}_{d_{\mathbf{t}_i}}, \cdots, \overline{\mathbb{D}}^{(\beta_m)}_{d_{\mathbf{t}_i}} \mathbf{x}_{d_{\mathbf{t}_i}}, \overline{\mathbb{D}}^{(\gamma_1)}_{d_{\mathbf{t}_i}} \mathbf{x}_{d_{\mathbf{z}_{i,1}}}, \cdots, \overline{\mathbb{D}}^{(\gamma_1)}_{d_{\mathbf{t}_i}} \mathbf{x}_{d_{\mathbf{z}_{i,s}}}), \tag{47}$$

such that

$$[\mathbf{x}_{k d_{\mathbf{t}_i}}]_1 = [\mathbf{x}_{k d_{\mathbf{z}_1}}]_N, \quad k = 0, 1, \cdots, n. \tag{48}$$

where $\mathbf{t}_i$ and $\mathbf{z}_{i,k}$ are the N number of discretized points in $[0, i\tau_1]$ and $[-\tau_k, -\tau_k + i\tau_1]$, $i = 1, 2, \cdots, n$, respectively, and $\mathbf{f}_{d_{\mathbf{t}_i}}$ is the discretized matrix of $\mathbf{f}(\cdot)$ at $\mathbf{t}_i$.

4 Numerical Stability

Studying the stability region of an integration method is a criterion to characterize its performance. The stability domain can be generally studied by solving a simple linear scalar differential equation.

Definition 4.1 ([29]). The numerical stability of a fractional spectral collocation method is tested by solving the following autonomous linear time-invariant FDE

$$ {}_0^C\mathcal{D}_t^{\alpha}[x(t)] + \lambda x(t) = 0, \quad \alpha \in (0,1], \tag{49} $$

with $x(0) = x_0 \in \mathbb{R}$ and $\lambda \in \mathbb{C}$. The exact solution of this equation is given by the Mittag-Leffler function as $x(t) = x_0 E_{\alpha,\alpha}(-\lambda t^{\alpha})$ which is asymptotically stable if $\arg(\lambda) > \alpha\frac{\pi}{2}$ [62].

According to Proposition 3.2 and the proposed discretization operators, the solution of Eq. (49) at the CGL collocation points $\mathbf{t}$ in $[0,\tau]$ is obtained by the state transition matrix T_{d_t}, i.e.

$$ T_{d_t} = \left(\overline{\mathbb{D}}_{d_t}^{\alpha} + \lambda \bar{I}_N\right)^{-1} J, \tag{50} $$

where $\bar{I}_N$ is a $N \times N$ identity matrix with its first element sets to zero and J is a $N \times N$ zero matrix whose first row is modified as $[0, 0, \cdots, 0, 1]$.

If $\alpha = 1$, since ${}_0^C\mathcal{D}_t^1[\cdot] \equiv d/dt$ and $\tilde{\mathbb{D}}_{d_t}^1$ are local operator, there exist a unique monodromy matrix $\mathcal{M}$ such that gives the solution $\mathbf{x}_j$ in jth interval $[(j-1)T, jT]$ as

$$ \mathbf{x}_{d_{t_j}} = \mathcal{M}^j \mathbf{x}_0, \tag{51} $$

The solution converges to zero if $\rho(\mathcal{M}) < 1$. Furthermore, the spectral radius depends on the adjustable parameters τ and N. Figure 3-a and -b demonstrate the stability domain by using the FCC method and the fractional finite difference differentiation matrix to solve Eq. (49), respectively. The FCC method gives the stability boundaries on the imaginary axis very straight in compare to the finite difference method.

For a fractional-order α, the numerical stability has been studied by using the short memory principle [29]. Figure 4 shows the stability boundaries given by this strategy for different values of the fixed memory τ and $N = 100$. It is shown that by increasing τ the stability boundaries are obtained more accurate. Improving the accuracy of obtaining the stability boundaries for a fractional-order case is achieved by increasing both τ and N.

Definition 4.2. The numerical stability of a fractional spectral collocation method for solving FDDEs is tested by solving the following linear time-invariant scalar FDDE with a single delay

$$ {}_0^C\mathcal{D}_t^{\alpha}[x(t)] = ax(t) + bx(t-\tau), \quad 0 \le \alpha \le 1, \tag{52} $$

subject to initial function $\phi(t)$, $t \in [-\tau, 0]$, where a and $b \in \mathbb{R}$.

Proposition 4.1. *The approximate stability boundaries of FDDE (52) is given by analyzing the spectral radius of its approximated monodromy matrix defined as*

$$ \tilde{\mathcal{M}} = \left(\overline{\mathbb{D}}_{d_t}^{\alpha} - a\bar{I}_N\right)^{-1} (b\bar{I}_N + J). \tag{53} $$

Moreover, the FCC method is numerically stable for FDDE (52) if and only if the spectral radius of the approximated monodromy matrix locates in the unite circle for large enough values of N and τ, or α's close to 1.

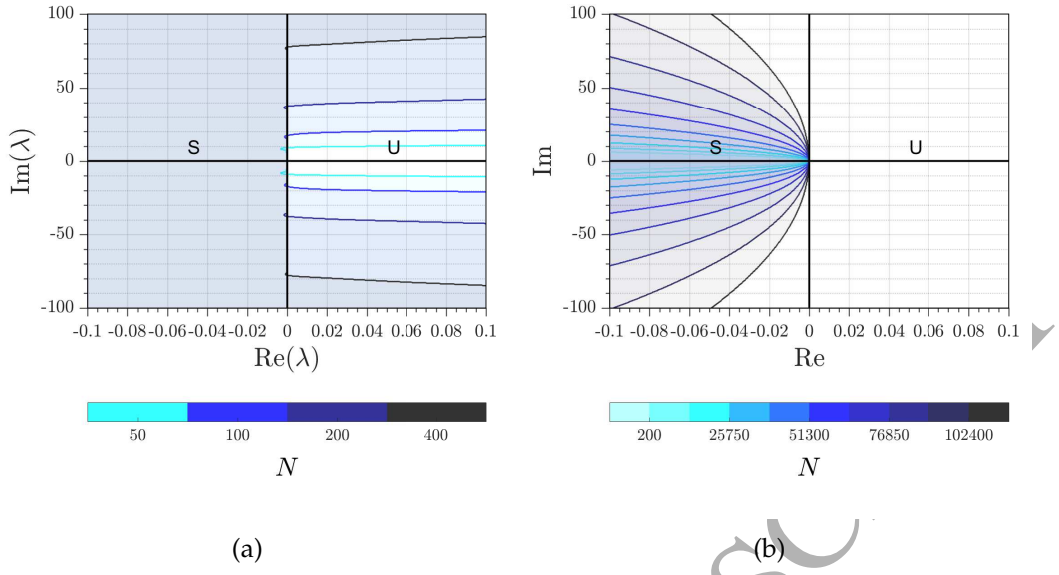

(a) (b)

Figure 3: The stability region of the FCC method and the finite difference method for Eq. (49) for different values of N when $\alpha = 1$ and $\tau = 1$. U (shaded regions) and S denote the unstable and stable region, respectively.

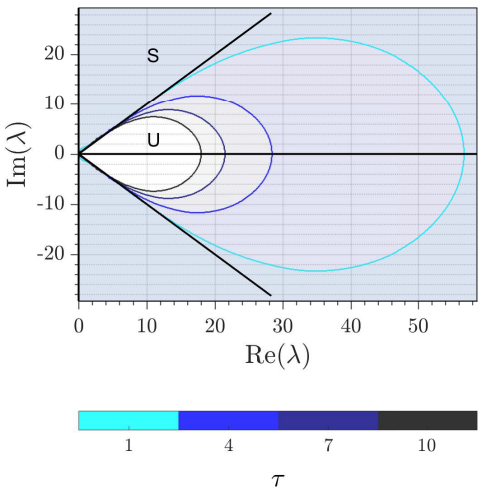

Figure 4: The stability region of the spectral numerical method for different values of τ when $\alpha = 0.5$ and $N = 100$. Inside the stability boundaries is unstable. The black lines shows the exact stability boundaries given by Matignon's theorem. U (shaded regions) and S denote the unstable and stable region, respectively.

Proof. According to Proposition 3.4, if $\alpha = 1$, then there exists a unique monodromy matrix $\mathcal{M}$ such that gives the solution $\mathbf{y}_k$ in kth interval $[(k-1)\tau, k\tau]$ as

$$\mathbf{y}_k = \mathcal{M}^k \mathbf{w}_0. \tag{54}$$

Thus, the solution converges to zero if and only if $\rho(\mathcal{M}) < 1$ where ρ is the spectral radius of the discretized monodromy matrix $\mathcal{M}$. For a fractional-order α, the main concern here is the nonlocal property of fractional derivate operators due to its fixed lower terminal. The short memory principle can be used to obtained the approximated solution explicitly by an approximated monodromy matrix. Moreover, the short-memory principle states that the solution of a fractional derivative can be approximated only by storing the most recent history of the function. Furthermore, if the lower terminal of the Caputo differentiation operator sets to be shorter in τ, then the error bound is

$$\left\| {}_0^C\mathcal{D}_t^\alpha [x(t)] - {}_{t-\tau}^C\mathcal{D}_t^\alpha [x(t)] \right\| \leq C \left(t^{1-\alpha} - \tau^{1-\alpha} \right) / \Gamma(2-\alpha), \tag{55}$$

where $C = \sup_{t \in [0,,(n-1)\tau]} |dx(t)/dt|$. It is noticed that the approximation improves when $\alpha \to 1$ or $\tau \to t$. Increasing τ results in obtaining the kth solution more accurate. Consequently, the approximated solution can be obtained by the approximated monodromy matrix as

$$\mathbf{y}_j \approx \tilde{\mathcal{M}}^k \mathbf{w}_0. \tag{56}$$

Therefore, the necessary and sufficient condition for the origin of system (52) to be asymptotically stable is that all the eigenvalues of $\tilde{\mathcal{M}}$ lie inside the unit circle for large enough values of N and τ, or α's close to 1. □

Comparing the numerical stability regions in the parametric plane $a - b$ with its analytical solution can be used to study the numerical stability of the method. For this purpose, the characteristic equation of FDDE (52) is

$$s^\alpha = a + \lambda e^{-\tau s} b. \tag{57}$$

The stability boundaries of FDDE (52) in the parametric plane $a - b$ can be derived by setting $\lambda = i\omega$, $\omega \in \mathbb{R}$, in which ω is the solution of

$$(i\omega)^\alpha - a - be^{-i\omega\tau} = \omega^\alpha e^{i\alpha\frac{\pi}{2}} - a - be^{-i\omega\tau} = 0. \tag{58}$$

Since this equation cannot be solved explicitly, the intersection point of the stability boundaries (b^*) with b-axis can be studies. The solution b^* is obtained by resolving Eq. (58) into real and imaginary parts by setting $a = 0$, i.e.

$$\omega^\alpha \cos\left(\alpha\frac{\pi}{2}\right) = b^* \cos(\omega\tau), \tag{59a}$$

$$\omega^\alpha \sin\left(\alpha\frac{\pi}{2}\right) = -b^* \sin(\omega\tau). \tag{59b}$$

One solution is $b^* = 0$ for $\omega = 0$, and the other solution is $b^* = -\omega^\alpha$ where $\omega\tau = (2-\alpha)\pi/2$. In addition, the line $a = -b$ is an invariant stability boundary for the FDDE (52) as it is independent of the fractional order when $\omega = 0$. Figure 5 shows the nonzero solution of the b^* for different fractional orders and delays. For $\alpha \to 0$, we have $b^* = -1$, and for $\alpha = 1$, we have $b^* = -\frac{\pi}{2\tau}$.

Figure 6 shows the approximated stability boundaries of FDDE (52) in the parametric plane $a - b$ by analyzing its approximated monodromy matrix. The shaded regions are the stability boundaries, and the filled circles show the analytical solution of the boundary intersections with the b-axis given in Eq. (59). For small values of the fractional orders, the intersection points do not exactly overlap with the analytical results due to error associated with the short memory principle. However, by increasing the fractional order, the approximation improves and becomes closer to the analytical solution.

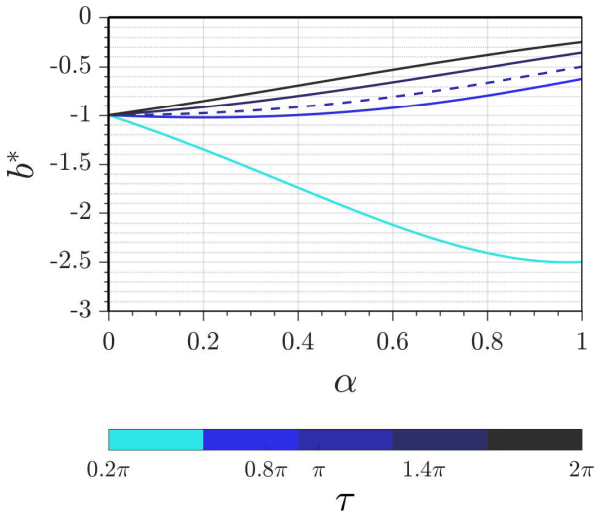

Figure 5: The analytical solution of the stability boundary intersection b^* with the b-axis for the fractional Hayes equation for different fractional orders and time-delays.

5 Convergence and Error Estimates

In this section, the convergence and error estimation of the approximated solution of the system of nonlinear FDEs (11) are derived. In addition, the basic definitions in the concept of the polynomial interpolation and Sobolev spaces are given in order to discuss error estimates for the proposed framework. The results of this section are derived for the FCC method at the CGL points, which can be extended for the other types of collocation points.

Definition 5.1. Let $\Omega \subset \mathbb{R}^n$ and $\mathbf{x} = [x_1, \cdots, x_n]^T$, $x_i \in \mathbb{R}$. Then, $L^2_w(\Omega)$ denotes the space of square-integrable functions $f(\mathbf{x})$ in Ω, i.e.,

$$L^2_w(\Omega) = \{f(\mathbf{x}) : \Omega \to \mathbb{R} | f(\mathbf{x}) \text{ is measurable and } \|f(\mathbf{x})\|_{L^2_w(\Omega)} < \infty\}, \tag{60}$$

where the corresponding norm $\|f(\mathbf{x})\|_{L^2_w(\Omega)}$ is defined by

$$\|f(\mathbf{x})\|_{L^2_w(\Omega)} = \sqrt{\langle f(\mathbf{x}), f(\mathbf{x})\rangle_{L^2_w(\Omega)}}, \tag{61}$$

and the inner product $\langle f(\mathbf{x}), f(\mathbf{x})\rangle_{L^2_w(\Omega)}$ is defined as

$$\langle f(\mathbf{x}), g(\mathbf{x})\rangle_{L^2_w(\Omega)} = \int_\Omega f(\mathbf{x}) g(\mathbf{x}) w(\mathbf{x}) d\mathbf{x}. \tag{62}$$

Definition 5.2. Let Ω be an open domain in $\mathbb{R}^n$ with the nonnegative multi-index $\boldsymbol{s} = \{s_1, \cdots, s_n\}$, $s_i \in \mathbb{Z}^+$, $i = 1, 2, \cdots, n$, and $s = \sum_{i=1}^n s_i$. Space $W^k_p(\Omega)$ is the Sobolev space of all functions $f(\mathbf{x})$ on an open domain Ω such that $f(\mathbf{x})$ and all its weak derivatives up to the order k are in the Lebesgue space $L^p(\Omega)$. That is

$$W^k_p(\Omega) = \{f(\mathbf{x}) \in L^p(\Omega) : \forall s,\ 0 \le s \le k, D^s f(\mathbf{x}) \in L^p(\Omega)\}, \tag{63}$$

where

$$D^s f(\mathbf{x}) = \frac{\partial^s f(\mathbf{x})}{\partial^{s_1} x_1 \partial^{s_2} x_2 \cdots \partial^{s_n} x_n}, \tag{64}$$

and the norm associated with it is

$$\|f(\mathbf{x})\|_{L^p(\Omega)} = \int_\Omega |f(\mathbf{x})|^p d\mathbf{x}. \tag{65}$$

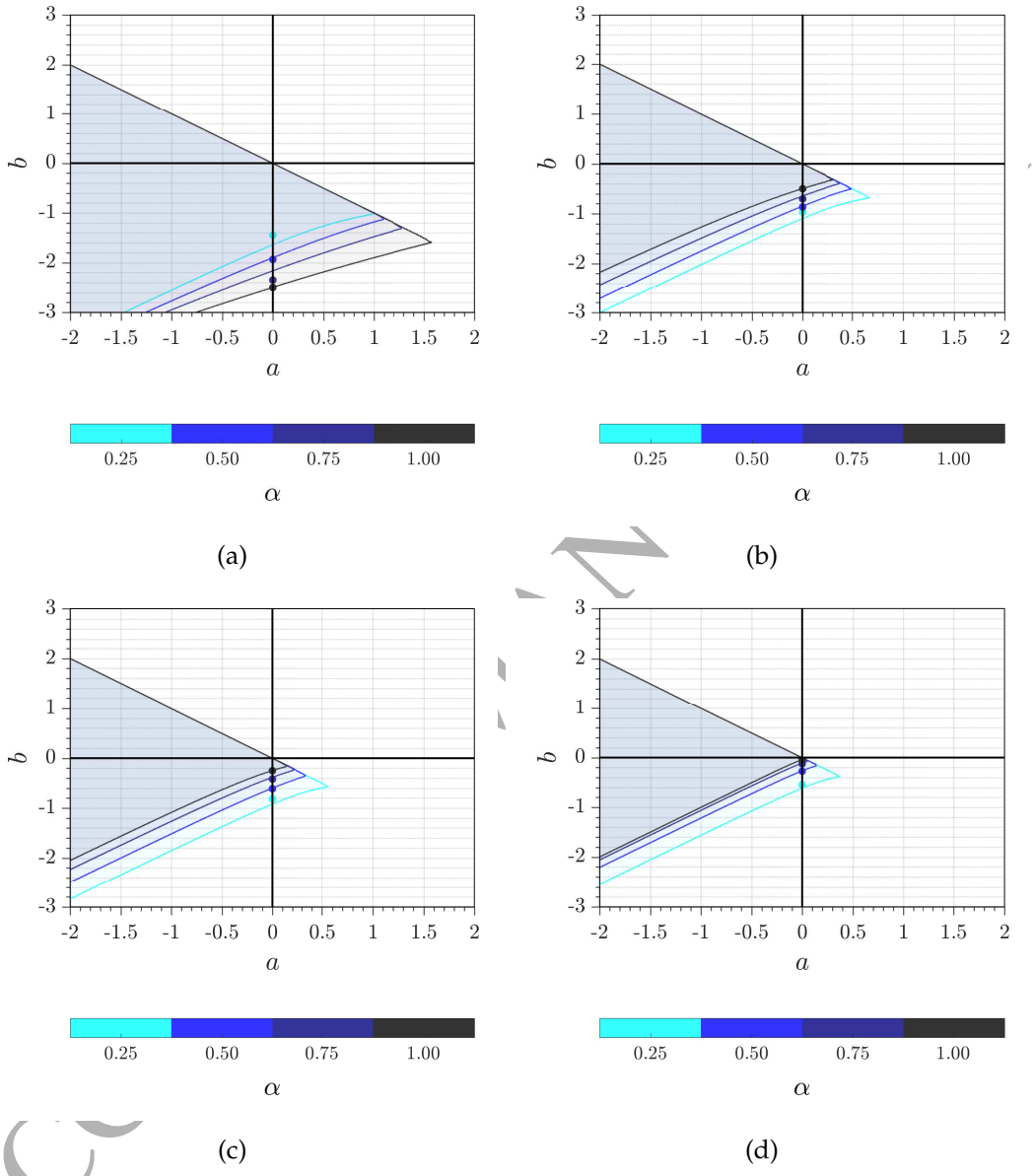

Figure 6: The stability region of FDDE (52) by using 100 CGL collocation points for different values of α and (a) $\tau = 0.2\pi$, (b) $\tau = \pi$, (c) $\tau = 2\pi$, and (d) $\tau = 10\pi$. The shaded regions indicate the stable boundaries, and the filled circles show the analytical solution of the b-axis stability boundary intersections.

When $p = 2$, then the Sobolev space $W_2^k(\Omega)$ is denoted by $H^k(\Omega)$. This space is a Hilbert space for the inner product

$$\langle f(\mathbf{x}), g(\mathbf{x})\rangle_{k,\Omega} = \sum_{s=0}^{k} \langle D^s f(\mathbf{x}), D^s g(\mathbf{x})\rangle_{L_2(\Omega)}. \tag{66}$$

$W_w^r(\Omega)$ is a Hilbert space when it is associated with the following norm and seminorm

$$\|f(\mathbf{x})\|_{W_w^r(\Omega)} = \left(\sum_{k=0}^{r} \left\|D^k f(\mathbf{x})\right\|^2_{L_w^2(\Omega)}\right)^{1/2}, \tag{67a}$$

$$|f(\mathbf{x})|_{W_w^{r;N}(\Omega)} = \left(\sum_{k=\min\{r,N+1\}}^{r} \left\|D^k f(\mathbf{x})\right\|^2_{L_w^2(\Omega)}\right)^{1/2}. \tag{67b}$$

Consequently, it can be shown that $W_w^r(\Omega) \subset W_w^{r-1}(\Omega) \subset \cdots W_w^2(\Omega) \subset W_w^1(\Omega) \subset W_w^0(\Omega) \equiv L_w^2(\Omega)$.

Theorem 5.1 ([63]). *Let $\mathbb{T}_N$ define the space of all Chebyshev polynomials $T_i(\xi)$, $0 = 1, 2, \cdots, N$, which are orthogonal and complete in $L_w^2(\Lambda)$, $\Lambda = [-1, 1]$, where $w(\xi) = 1/\sqrt{1-\xi^2}$. In addition, $\mathcal{P}_N : L_w^2(\Lambda) \to \mathbb{T}_N$ denotes an orthogonal projection for any $x(t) \in L_w^2(\Lambda)$. For all $x(\xi) \in L_w^2(\Lambda)$, $\mathcal{P}_N x(\xi)$ is a Chebyshev interpolant at the CGL collocation points $\boldsymbol{\xi} = [\xi_0 = -1, \xi_1, \cdots, \xi_{N-1} = 1]$ such that*

$$\mathcal{P}_N x(\xi_i) = x(\xi_i), \quad i = 0, 1, \cdots, N-1, \tag{68}$$

and

$$\|\mathcal{P}_N x(\xi) - x(\xi)\|_{L_w^2(\Lambda)} \to 0 \quad \text{as} \quad N \to \infty. \tag{69}$$

In addition, for any $x(\xi), y(\xi) \in \mathbb{T}_N$, we have

$$\langle \mathcal{P}_N x(y), y(\xi)\rangle_{L_w^2(\Lambda)} = \langle x(\xi), y(\xi)\rangle_{L_w^2(\Lambda)}. \tag{70}$$

Proposition 5.1 (Eq. (5.3.2) in [63]). *For any $\phi \in \mathcal{P}_{N-1}(\Lambda)$, we have*

$$\|\phi\|_{L_w^2(\Lambda)} \le \|\phi\|_N \le \sqrt{2}\|\phi\|_{L_w^2(\Lambda)}, \tag{71}$$

where

$$\|\phi\|_N = \left(\sum_{i=0}^{N-1} \phi^2(\xi_i) w(\xi_i)\right)^{1/2}. \tag{72}$$

.

Theorem 5.2 (Sec 5.5.2-3 in [63]). *Suppose $H_w^r(\Lambda)$, $r \ge 1$, is the Hilbert space associated with the following Sobolev norm $\|x\|_{H_w^r(\Lambda)}$ and seminorm $|x|_{H_w^{r;m}(\Lambda)}$*

$$\|x(\xi)\|_{H_w^r(\Lambda)} = \left(\sum_{i=0}^{r} \left\|\partial_t^i x(\xi)\right\|^2_{L_w^2(\Lambda)}\right)^{1/2}, \tag{73a}$$

$$|x(\xi)|_{H_w^{r;m}(\Lambda)} = \left(\sum_{i=\min\{r,m+1\}}^{r} \left\|\partial_\xi^i x(\xi)\right\|^2_{L_w^2(\Lambda)}\right)^{1/2}. \tag{73b}$$

For all $x(\xi) \in H^r_w(\Lambda)$ with $1 \le l \le r$, the truncation error $e_N(\xi) = x(\xi) - \mathcal{P}_N x(\xi)$ holds the following inequalities

$$\|e_N(\xi)\|_{L^2_w(\Lambda)} \le CN^{-r}|x(\xi)|_{H^{r;N}_w(\Lambda)}, \tag{74a}$$

$$\|e_N(\xi)\|_{H^r_w(\Lambda)} \le CN^{-r}\|x(\xi)\|_{H^r_w(\Lambda)}, \tag{74b}$$

$$\|e_N(\xi)\|_{L^\infty_w(\Lambda)} \le CN^{1/2-r}|x(\xi)|_{H^{r;N}_w(\Lambda)}, \tag{74c}$$

where $C \in \mathbb{R}^+$ and $\|\cdot\|_{L^\infty_w(\Lambda)} = \sup_\Lambda |\cdot|$.

Lemma 5.1. *Let $\Omega = [a, b]$ and $h = b - a$. For all $x(t) \in H^r_\psi(\Omega)$ with $1 \le r < N$, the truncation error $e_N(t) = x(t) - \mathcal{P}_N x(t)$ holds the following inequalities*

$$\|e_N(t)\|_{L^2_\psi(\Omega)} \le C\left(\frac{N}{h}\right)^{-r}|x(t)|_{H^{r;N}_\psi(\Omega)}, \tag{75a}$$

$$\|e_N(t)\|_{H^r_w(\Lambda)} \le C\left(\frac{N}{h}\right)^{-r}\|x(t)\|_{H^r_w(\Lambda)}, \tag{75b}$$

$$\|e_N(t)\|_{L^\infty_\psi(\Omega)} \le C\left(\frac{N}{h}\right)^{1/2-r}|x(t)|_{H^{r;N}_\psi(\Omega)}. \tag{75c}$$

Proof. By considering that $t = \frac{h}{2}(\xi + 1) + a$ and $\psi(t) = w(\frac{h}{2}(\xi + 1) + a)$, we have

$$\begin{aligned}
\|e_N(t)\|^2_{L^2_\psi(\Omega)} &= \int_\Omega e^2_N(t)\psi(t)dt = \frac{h}{2}\|e_N(\xi)\|^2_{L^2_w(\Lambda)} \le \frac{h}{2}C^2N^{-2r}|x(\xi)|^2_{H^{r;N}_w(\Lambda)} \\
&\le \frac{h}{2}C^2N^{-2r}\sum_{i=\min\{r,N+1\}}^{r}\left\|\partial^i_\xi x(\xi)\right\|^2_{L^2_w(\Lambda)} \\
&\le h^{-2r}C^2N^{-2r}\sum_{i=\min\{r,N+1\}}^{r}\left\|\partial^i_t x(t)\right\|^2_{L^2_\psi(\Omega)}.
\end{aligned} \tag{76}$$

Taking the square root of the both sides completes the proof of the first inequality. Similarly, the second and third equalities can be proved. □

Definition 5.3. Let $\mathbb{D} \subset \mathbb{R}^n$ be an bounded closed set, and let $f(\mathbf{x}) \in \mathcal{C}(\mathbb{D})$. Then $f(\mathbf{x})$ is a Lipschitz function such that for all $\mathbf{x}, \mathbf{y} \in \mathbb{D}$ we have

$$|f(\mathbf{x}) - f(\mathbf{y})| \le l_p\|\mathbf{x} - \mathbf{y}\|_q, \tag{77}$$

where $\frac{1}{p} + \frac{1}{q} = 1$, $1 \le p, q \le \infty$, $l_p = \sup_{x\in\mathbb{D}}\{\|\Delta f(\mathbf{x})\|_p\}$ is the Lipschitz constant in which $\Delta f(\mathbf{x}) = (\partial_{x_1} f, \cdots, \partial_{x_n} f)$.

Lemma 5.2. *Let $f(\mathbf{x})$ be Lipschitz in $\Omega \subset \mathbb{R}$ such that $|f(\mathbf{x}) - f(\mathbf{y})| \le L_f\|\mathbf{x} - \mathbf{y}\|_{L^2(\Omega)}$. Then for all $x, y \in \Omega$ we have*

$$\|f(\mathbf{x}) - f(\mathbf{y})\|_{L^2_w(\Omega)} \le L_f\|\mathbf{x} - \mathbf{y}\|_{L^2_w(\Omega)}. \tag{78}$$

Proof. Using the definition of the pth weighted norm gives

$$\begin{aligned}
\|f(\mathbf{x}) - f(\mathbf{y})\|^2_{L^2_w(\Omega)} &= \int_\Omega |f(\mathbf{x}) - f(\mathbf{y})|^2 w(\mathbf{x})d\mathbf{x} \\
&\le L^2_f\int_\Omega |\mathbf{x} - \mathbf{y}|^2 w(\mathbf{x})d\mathbf{x} \\
&\le L^2_f\|\mathbf{x} - \mathbf{y}\|^2_{L^2_w(\Omega)}.
\end{aligned} \tag{79}$$

This completes the proof of Lemma 5.2. □

Lemma 5.3 (Lemma 2.1 in [53]). *The fractional integration operator ${}_a^C\mathcal{J}_t^\alpha[\cdot]$ with $\alpha > 0$ is bounded in $L^p(\Omega)$, $1 \le p \le \infty$, $\Omega = [a,b]$. That is*

$$\left\| {}_a^C\mathcal{J}_t^\alpha[x(t)] \right\|_{L^p(\Omega)} \le K \|x(t)\|_{L^p(\Omega)}, \tag{80}$$

where $x(t) \in \mathbb{R}$ and $K = \frac{(b-a)^\alpha}{\Gamma(\alpha+1)}$.

Lemma 5.4. *Let $\alpha > 0$ and $x(a) = \partial_t x(a) = \cdots = \partial_t^{r+\lceil\alpha\rceil} x(a) = 0$, then*

$$\partial_t^r \, {}_a^C\mathcal{J}_t^\alpha[x(t)] = {}_a^C\mathcal{J}_t^\alpha[\partial_t^r x(t)], \tag{81a}$$
$$\partial_t^r \, {}_a^C\mathcal{D}_t^\alpha[x(t)] = {}_a^C\mathcal{D}_t^\alpha[\partial_t^r x(t)]. \tag{81b}$$

Proof. The proof can be obtained by applying the integration by part on the fractional derivative of $x(t)$ defined in Definition. 2.4. □

Theorem 5.3. *Let $\Omega = [a,b]$, $0 < \lceil\alpha\rceil - 1 \le \alpha \le \lceil\alpha\rceil$. For any $x(t) \in W_w^{r+\lceil\alpha\rceil}(\Omega)$, $r \ge 0$, with $x(a) = \partial_t x(a) = \cdots = \partial_t^{r+\lceil\alpha\rceil} x(a) = 0$, we have*

$$\left\| {}_a^C\mathcal{D}_t^\alpha[x(t)] \right\|_{W_w^r(\Omega)} \le C \left\| \partial_t^{\lceil\alpha\rceil} x(t) \right\|_{W_w^r(\Omega)} = C \|x(t)\|_{W_w^{r+\lceil\alpha\rceil}(\Omega)}, \tag{82}$$

where $C = \frac{(b-a)^{\lceil\alpha\rceil-\alpha+1}}{\Gamma(\lceil\alpha\rceil-\alpha+1)\sqrt{(2\lceil\alpha\rceil-2\alpha+1)}}$.

Proof. According to the definition of the Sobolev norm given in Definition 5.2 and Lemma 5.4, we have

$$\begin{aligned} \left\| {}_a^C\mathcal{D}_t^\alpha[x(t)] \right\|^2_{W_w^r(\Omega)} &= \sum_{k=0}^r \left\| \partial_t^k \, {}_a^C\mathcal{D}_t^\alpha[x(t)] \right\|^2_{L^2_w(\Omega)} = \sum_{k=0}^r \left\| {}_a^C\mathcal{D}_t^\alpha[\partial_t^k x(t)] \right\|^2_{L^2_w(\Omega)} \\ &= \sum_{k=0}^r \int_\Omega \left(\frac{1}{\Gamma(\lceil\alpha\rceil-\alpha)} \int_a^t \frac{\partial_\tau^{k+\lceil\alpha\rceil} x(\tau)}{(t-\tau)^{\alpha+1-\lceil\alpha\rceil}} d\tau \right)^2 w(t) dt. \end{aligned} \tag{83}$$

Using the integration by part yields

$$\left\| {}_a^C\mathcal{D}_t^\alpha[x(t)] \right\|^2_{W_w^r(\Omega)} = \sum_{k=0}^r \int_\Omega \left(\frac{1}{\Gamma(\lceil\alpha\rceil-\alpha+1)} \int_a^t \partial_\tau^{k+\lceil\alpha\rceil+1} x(\tau)(t-\tau)^{\lceil\alpha\rceil-\alpha} d\tau. \right)^2 w(t) dt \tag{84}$$

Now, by using the Cauchy-Schwarz inequality

$$\begin{aligned} \left\| {}_a^C\mathcal{D}_t^\alpha[x(t)] \right\|^2_{W_w^r(\Omega)} &\le \sum_{k=0}^r C^2 \int_\Omega \left(\partial^{k+\lceil\alpha\rceil} x(t) \right)^2 w(t) dt \\ &\le C^2 \sum_{k=0}^r \int_\Omega \left(\partial^k \partial^{\lceil\alpha\rceil} x(t) \right)^2 w(t) dt \\ &\le C^2 \left\| \partial^{\lceil\alpha\rceil} x(t) \right\|^2_{W_w^r(\Omega)} = C^2 \|x(t)\|^2_{W_w^{r+\lceil\alpha\rceil}(\Omega)}. \end{aligned} \tag{85}$$

This ends the proof of Theorem 5.3. □

Theorem 5.4. *Let $\Omega = [0, T]$ and $x_i(t), x_i(t-\tau_j), f_i(\cdot) \in W_\psi^r(\Omega)$, $i = 1, 2, \cdots, n$, $j = 1, 2 \cdots, s$. The functions $f_i(\cdot)$, $i = 1, \cdots, n$, are Lipschitz continuous with respect to $\mathbf{x}(t)$, ${}_0^C\mathcal{D}_t^{\beta_i}[\mathbf{x}(t)]$, and ${}_0^C\mathcal{D}_t^{\beta_j}[\mathbf{x}(t-\tau_j)]$, $i = 1, \cdots, m$, $\nu_1, \cdots, s$, with the Lipschitz constant $K_i > 0$.*

(I) For $T < \tau_1$, the approximated solution in $\Omega = [0, \tau_1]$ obtained by the use of the FCC method converges and has a spectral convergence with the error bound

$$\|e_i\|_{L_\psi^2(\Omega)} \leq K_i \left(\frac{N}{h}\right)^{-r} \left(L_x \sum_{j=1}^{n} C_{1_j} |x_j|_{H_\psi^{r;N}(\Omega)} + C_4 |f_i|_{H_\psi^{r;N}(\Omega)}\right) +$$

$$K_i \left(\frac{N}{h}\right)^{-1} \left(\sum_{k=0}^{m}\sum_{j=1}^{n} C_{b_k} L_{b_k} C_{2_j} |x_j(t)|_{H_\psi^1(\Omega)} + \sum_{k=0}^{s}\sum_{j=1}^{n} C_{v_k} L_{v_k} C_{3_j} |x_j(t-\tau_k)|_{H_\psi^1(\Omega)}\right), \tag{86}$$

where $L_x, L_{b_k}, L_{v_k} \in \mathbb{R}^+$, $C_{b_k} = \frac{(b-a)^{2-\beta_k}}{\Gamma(1-\beta_k)\sqrt{(3-2\beta_k)}}$, and $C_{v_k} = \frac{(b-a)^{2-\nu_k}}{\Gamma(1-\nu_k)\sqrt{(3-2\nu_k)}}$, $C_{k_j} > 0$, $k = 1, 2, 3$, $j = 1, 2, \cdots, n$, and $C_4 > 0$.

(II) If $T > \tau_1$, N is chosen large enough, and $x(t) \in W_\psi^4(\Omega)$, then the error of the approximated solution in $\Omega = [0, T]$ obtained by the use of the FCC method enhanced with the PCHIP internal interpolation is $O(h^4)$ where $h = \max_{i=0,\cdots,N-1} |t_i - t_{i-1}|$.

Proof. Without loss of generality, we assume that the initial condition of the system of nonlinear FDEs in Eq. (11) is zero. In the case of nonzero initial conditions, the following transformation can be used:

$$\mathbf{x}(t) = \mathbf{z}(t) + \mathbf{x}(0), \tag{87}$$

where $\mathbf{x}(0) = \mathbf{\Phi}(0)$.

The ith equation of the system of nonlinear FDEs in Eq. (11) is equivalent to

$$\begin{aligned} &x_i(t) = \\ &{}_0^C\mathcal{J}_t^{\alpha_i}[f_i(t, \mathbf{x}(t), {}_0^C\mathcal{D}_t^{\beta_1}[\mathbf{x}(t)], \cdots, {}_0^C\mathcal{D}_t^{\beta_m}[\mathbf{x}(t)], {}_0^C\mathcal{D}_t^{\nu_1}[\mathbf{x}(t-\tau_1)], \cdots, {}_0^C\mathcal{D}_t^{\nu_s}[\mathbf{x}(t-\tau_s)])]. \end{aligned} \tag{88}$$

Let $\mathcal{P}_N\mathbf{x}(t) = [\mathcal{P}_N x_1(t), \cdots, \mathcal{P}_N x_n(t)]^T$ and $\mathcal{P}_N\mathbf{f} = [\mathcal{P}_N f_1, \cdots, \mathcal{P}_N f_n]^T$ be the interpolation polynomial of the exact solution $\mathbf{x}(t)$ and $\mathbf{f}$ at the CGL point $\mathbf{t}_{d_t} = [t_0 = 0, t_1, \cdots, t_{N-1} = \tau_1]^T$ in $[0, \tau_1]$. Then, by using Eq. (11) we have

$$\begin{aligned} &\mathcal{P}_N x_i(t) = {}_0^C\mathcal{J}_t^{(\alpha_1,\cdots,\alpha_n)}[f_i(t, \mathcal{P}_N\mathbf{x}(t), {}_0^C\mathcal{D}_t^{\beta_1}[\mathcal{P}_N\mathbf{x}(t)], \cdots, {}_0^C\mathcal{D}_t^{\beta_m}[\mathcal{P}_N\mathbf{x}(t)], \\ &{}_0^C\mathcal{D}_t^{\nu_1}[\mathcal{P}_N\mathbf{x}(t-\tau_1)], \cdots, {}_0^C\mathcal{D}_t^{\nu_s}[\mathcal{P}_N\mathbf{x}(t-\tau_s)])]. \end{aligned} \tag{89}$$

Suppose $\mathbf{e}(t) = \mathbf{x}(t) - \mathcal{P}_N\mathbf{x}(t)$. Subtracting Eq. (89) from Eq. (88) results in

$$e_i = {}_0^C\mathcal{J}_t^{\alpha_i}\left[I_1 + I_2\right]. \tag{90}$$

where

$$\begin{aligned} &I_1 = \\ &f_i(t, \mathbf{x}(t), {}_0^C\mathcal{D}_t^{\beta_1}[\mathbf{x}(t)], \cdots, {}_0^C\mathcal{D}_t^{\beta_m}[\mathbf{x}(t)], {}_0^C\mathcal{D}_t^{\nu_1}[\mathbf{x}(t-\tau_1)], \cdots, {}_0^C\mathcal{D}_t^{\nu_s}[\mathbf{x}(t-\tau_s)]) - \\ &f_i(t, \mathcal{P}_N\mathbf{x}(t), {}_0^C\mathcal{D}_t^{\beta_1}[\mathcal{P}_N\mathbf{x}(t)], \cdots, {}_0^C\mathcal{D}_t^{\beta_m}[\mathcal{P}_N\mathbf{x}(t)], {}_0^C\mathcal{D}_t^{\nu_1}[\mathcal{P}_N\mathbf{x}(t-\tau_1)], \cdots, {}_0^C\mathcal{D}_t^{\nu_s}[\mathcal{P}_N\mathbf{x}(t-\tau_s)]), \end{aligned} \tag{91a}$$

$$\begin{aligned} &I_2 = \\ &\mathcal{P}_N f_i(t, \mathcal{P}_N\mathbf{x}(t), {}_0^C\mathcal{D}_t^{\beta_1}[\mathcal{P}_N\mathbf{x}(t)], \cdots, {}_0^C\mathcal{D}_t^{\beta_m}[\mathcal{P}_N\mathbf{x}(t)], {}_0^C\mathcal{D}_t^{\nu_1}[\mathcal{P}_N\mathbf{x}(t-\tau_1)], \cdots, {}_0^C\mathcal{D}_t^{\nu_s}[\mathcal{P}_N\mathbf{x}(t-\tau_s)]) - \\ &f_i(t, \mathcal{P}_N\mathbf{x}(t), {}_0^C\mathcal{D}_t^{\beta_1}[\mathcal{P}_N\mathbf{x}(t)], \cdots, {}_0^C\mathcal{D}_t^{\beta_m}[\mathcal{P}_N\mathbf{x}(t)], {}_0^C\mathcal{D}_t^{\nu_1}[\mathcal{P}_N\mathbf{x}(t-\tau_1)], \cdots, {}_0^C\mathcal{D}_t^{\nu_s}[\mathcal{P}_N\mathbf{x}(t-\tau_s)]). \end{aligned} \tag{91b}$$

Using Lemma 5.3 gives

$$\|e_i\|_{L^2_\psi(\Omega)} \leq K_i \|I_1\|_{L^2_\psi(\Omega)} + K_i \|I_2\|_{L^2_\psi(\Omega)} \tag{92}$$

By using the Lipschitz condition for $f_i(\cdot)$, I_1 can be written as

$$\|I_1\|_{L^2_\psi(\Omega)} \leq L_x \|\mathbf{e}(t)\|_{L^2_\psi(\Omega)} + \sum_{k=0}^{m} L_{b_k} \left\| {}_0^C\mathcal{D}_t^{\beta_k} \mathbf{e}(t) \right\|_{L^2_\psi(\Omega)} + \sum_{k=0}^{s} L_{b_k} \left\| {}_0^C\mathcal{D}_t^{\nu_k} \mathbf{e}(t-\tau_k) \right\|_{L^2_\psi(\Omega)}. \tag{93}$$

Since $\|\cdot\|_{L^2_\psi(\Omega)} = \|\cdot\|_{H^0_\psi(\Omega)}$, $w(t) > 0$, Theorem 5.3 can be applied resulting in

$$\|I_1\|_{L^2_\psi(\Omega)} \leq L_x \sum_{j=1}^{n} \|e_j(t)\|_{L^2_\psi(\Omega)} + \sum_{k=0}^{m}\sum_{j=1}^{n} C_{b_k} L_{b_k} \|e_j(t)\|_{W^1_\psi(\Omega)} + \sum_{k=0}^{s}\sum_{j=1}^{n} C_{v_k} L_{v_k} \|e_j(t-\tau_k)\|_{W^1_\psi(\Omega)}. \tag{94}$$

In addition, according to Lemma 5.1, $\|e_j(t)\|_{L^2_\psi(\Omega)}$, $\|e_j(t)\|_{W^1_\psi(\Omega)}$, and $\|e_j(t-\tau_k)\|_{H^1_\psi(\Omega)}$ in the right-hand side of Eq. (94) can be bounded with Sobolev norms of $x_j(t)$ and $x_j(t-\tau_k)$. That is

$$\begin{aligned} \|I_1\|_{L^2_\psi(\Omega)} \leq K_i \left(\frac{N}{h}\right)^{-r} L_x \sum_{j=1}^{n} C_{1_j} |x_j|_{H^{r;N}_\psi(\Omega)} + \\ \left(\frac{N}{h}\right)^{-1} \left(\sum_{k=0}^{m}\sum_{j=1}^{n} C_{b_k} L_{b_k} C_{2_j} |x_j(t)|_{H^1_\psi(\Omega)} + \sum_{k=0}^{s}\sum_{j=1}^{n} C_{v_k} L_{v_k} C_{3_j} |x_j(t-\tau_k)|_{H^1_\psi(\Omega)} \right), \end{aligned} \tag{95}$$

Consequently, using Lemma 5.1 for $\|I_2\|_{L^2_\psi(\Omega)}$ in Eq. (91b), and substituting the obtained result along with the result of Eq. (95) into Eq. (92) yields the bounded error given in Eq. (86). This completes the proof of the first part of Theorem 5.4.

Let the error of the internal interpolation be denoted by ξ. To find the solution in Ω when $T > \tau_1$, this error is added to the delayed term in the last part of I_1. Therefore, the error of solution is obtained as the maximum of the interpolation error in Eq. (86) and ξ. In [64], it is shown that the approximation of $x(t)$ with the PCHIP has the error in $[t_{i-1}, t_i]$

$$\xi_i(t) = \frac{x^{(4)}(\zeta_i)}{4!}(t-t_{i-1})^2(t-t_i)^2, \quad i = 0, 1, \cdots, N-1, \tag{96}$$

where $\zeta_i \in [t_{i-1}, t_i]$. For non-equispaced points with step size of h_i, $i = 0, 1, \cdots, N-1$, the error is bounded by $\xi_i(t) \leq M_4 h^4/384$ where $M_4 = \max_{t_0 \leq \zeta \leq t_{N-1}} \left| x^{(4)}(\zeta) \right|$ and $h = \max_{i=0,\cdots,N-1} |t_i - t_{i-1}|$. As a result, the error of interpolation is smaller than that of the internal interpolation for large enough N, and hence the error of solution is $O(h^4)$. This ends the proof for the second part of Theorem 5.4. □

6 Numerical Simulations

In this section, the advantages of the FCC method are shown in several numerical examples. It is shown that the FCC method handles incommensurate order FDEs in noncanonical form as well as FDDEs with delays and time-varying coefficients. The FCC toolbox is available online, and it also includes all the following examples [50].

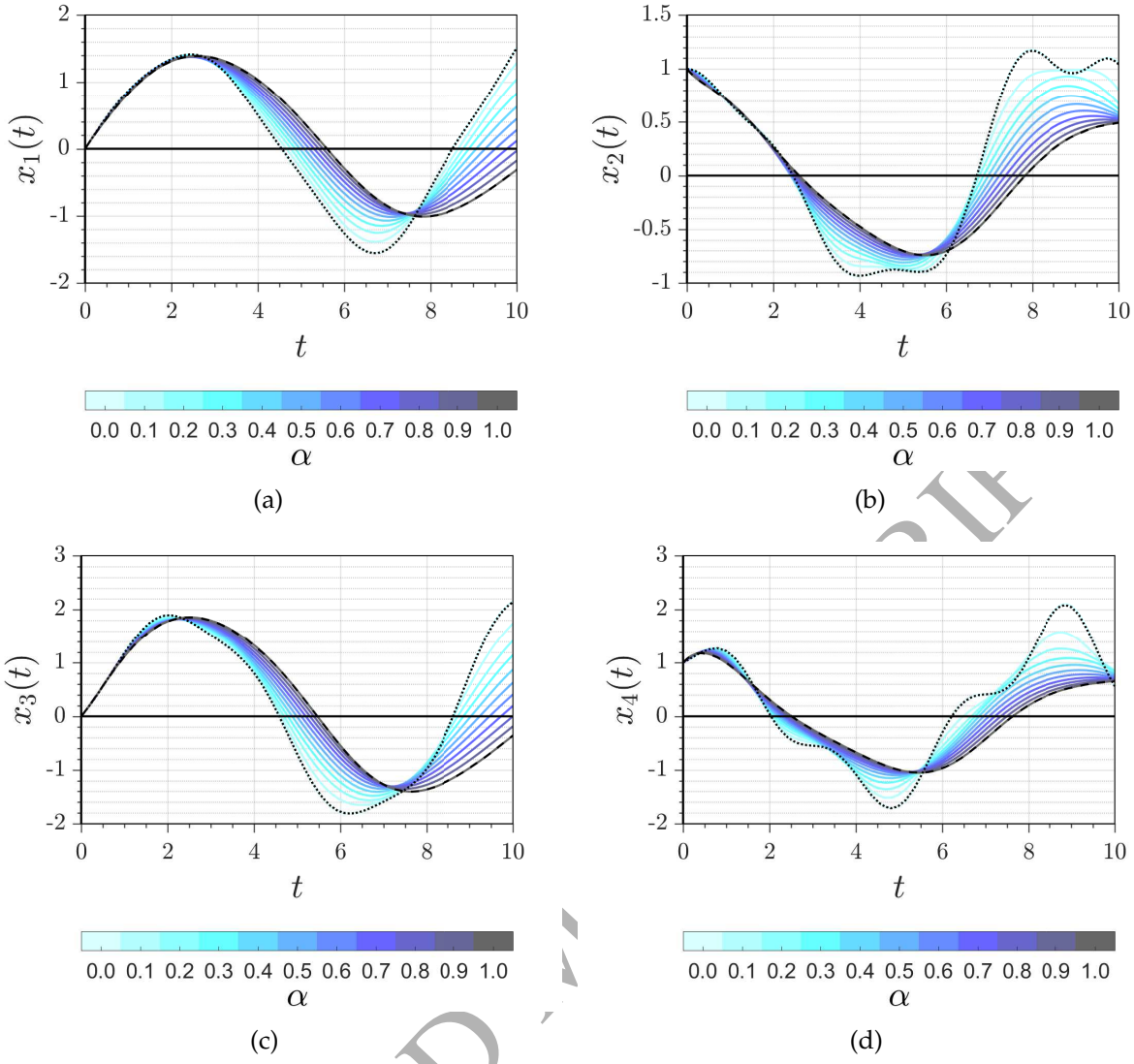

Figure 7: The numerical solution of Example 6.1 by using the FCC method for different values α. The dotted and dashed lines are the solution obtained by the `dde23`-solver in MATLAB when $\alpha = 0$ and $\alpha = 1$, respectively.

Example 6.1 (Beck's Column)**.** The FDDEs in Eq. (9) can be represented in the form of Eq. (41), i.e.

$$\dot{\mathbf{x}}(t) = \begin{bmatrix} 0 & 1 & 0 & 0 \\ \frac{\bar{P}}{2} - \frac{3\left(k + c_f\, {}_0^C\mathcal{D}_t^\alpha\right)}{2} & 0 & \left(k + c_f\, {}_0^C\mathcal{D}_t^\alpha\right) - \frac{\bar{P}}{2} & 0 \\ 0 & 0 & 0 & 1 \\ \frac{5\left(k + c_f\, {}_0^C\mathcal{D}_t^\alpha\right)}{2} - \frac{\bar{P}}{2} & 0 & \frac{3\bar{P}}{2} - 2\left(k + c_f\, {}_0^C\mathcal{D}_t^\alpha\right) & 0 \end{bmatrix} \mathbf{x}(t) + \begin{bmatrix} 0 & 0 & 0 & 0 \\ 0 & 0 & 0 & 0 \\ 0 & 0 & 0 & 0 \\ 0 & 0 & -\lambda\bar{P} & 0 \end{bmatrix} \mathbf{x}(t-\tau), \tag{97}$$

Let $k = 1$ N/m, $c = 1$ N/ms, $\lambda = 0.2$, $P_s = 1$ N, $P_d = 0.5$ N, $\Omega = 1.5$ rad/s, $\tau = 0.2$ sec, and $\mathbf{x}(t) = [t, 1, \sin(t), \cos(t)]^T$, $-\tau \le t \le 0$, in Eq. (97). The FCC method with 100 collocation points can be used to find its solution in $[0, 10]$. Figure 7 shows the response of the system (97) for different value of α. The obtained solutions by the use of the FCC method are compared to that obtained by the `dde23` in MATLAB when $\alpha = 0$ and 1. It shows that the solutions obtained for integer order α are similar to those obtained by the `dde23`.

Example 6.2 (Chaotic fractional system)**.** Consider the chaotic damped externally driven

pendulum with a dashpot

$$\ddot{x} + \mu \ {}_0^C\mathcal{D}_t^{\alpha} x + \omega^2 \sin x = F_0 \sin \Omega t, \tag{98}$$

where $\mu = 0.5$ is the damping coefficient, and the natural and external frequencies of the system are assumed to be $\omega = 1$ rad/s and $\Omega = \frac{2}{3}$ rad/s, respectively. The strength of the normalized driving torque F_0 is considered as the bifurcation parameter of the system. In [65], the dynamics of the system have been studied for $\alpha = 0.8$, and it has been shown that the system becomes chaotic after $F_0 > 1.052$. Inhere, the non-chaotic response $F_0 = 1.02$ is studied. Although the exact solution of Eq. (98) is not available, the convergence order respect to the number of collocation points can be approximated by using the two following criteria.

In the first criterion, the error of numerical solution is calculated by using a reference numerical solution obtained by a large number of collocation points or a small step size in finite difference methods. Furthermore, let $[\mathbf{x}_{d_{t_i}}]_{N_k}$ denote the discretized solution at the ith collocation point with the N_k number of collocation points. Then, the error is given by

$$\epsilon_{N_i} = \left\| [\mathbf{x}_{d_{t_i}}]_{N_i} - [\mathbf{x}_{d_{t_i}}]_{N_r} \right\|, \tag{99}$$

where N_r is the number of collocation points for the reference solution. Therefore, the convergence order in the first method is defined as

$$\mathcal{CO}_i^{(I)} = \frac{\log\left(\epsilon_{N_{i+1}} / \epsilon_{N_i}\right)}{\log\left(N_{i+1} / N_i\right)}. \tag{100}$$

In the second criterion, the convergence order is obtained by calculating the relative error of the solutions when the number of collocation points is increased by a factor of λ. Furthermore,the convergence order ν is defined by

$$\frac{[\mathbf{x}_{d_{t_i}}]_N - [\mathbf{x}_{d_{t_i}}]_{\lambda N}}{[\mathbf{x}_{d_{t_i}}]_{\lambda N} - [\mathbf{x}_{d_{t_i}}]_{\lambda^2 N}} = \frac{cN^{-\nu} - c(N\lambda)^{-\nu} + O(N^{-\nu-1})}{c(N\lambda)^{-\nu} - c(N\lambda^2)^{-\nu} + O(N^{-\nu-1})} = \lambda^{\nu} + O(N^{-1}), \tag{101}$$

where $c \in \mathbb{R}$ and $O(\cdot)$ is the big-O. Consequently, the convergence rate can be obtained by the following equation

$$\mathcal{CO}_i^{(II)} = \nu = \log_{\lambda}\left(\frac{[\mathbf{x}_{d_{t_i}}]_N - [\mathbf{x}_{d_{t_i}}]_{\lambda N}}{[\mathbf{x}_{d_{t_i}}]_{\lambda N} - [\mathbf{x}_{d_{t_i}}]_{\lambda^2 N}}\right). \tag{102}$$

The convergence order of finite difference methods must be constant in contrast to that of spectral methods which changes drastically because of their spectral property [13, 14]. For instance, Fig. 8 demonstrates the approximation error of the numerical solution of $\ddot{x}(t) + x(t) = 0$ with the initial conditions $x(0) = 1$ and $\dot{x}(0) = 0$ for $t \in [0, 4\pi]$. This differential equation is integrated by the FCC method and a finite difference method for different number of collocation points. In the FCC method, the error decreases exponentially by increasing the number of collocation points until it reaches to the machine precision, and after that fluctuates around zero. On the other hand, the approximation error obtained by the finite difference method reduces with a constant slope by increasing the number of collocation points where $N \approx h^{-1}$. Table 1 shows the calculated convergence order of the both methods by using the exact solution. In the spectral method, the convergence order decreases drastically and reaches to its minimum (indicated by the blue row), and after that fluctuates around zero (indicated by the red rows). Conversely, the convergence order of the finite difference method is about 2 for all the numbers of collocation points, i.e. $O(h^2) \equiv O(N^{-2})$.

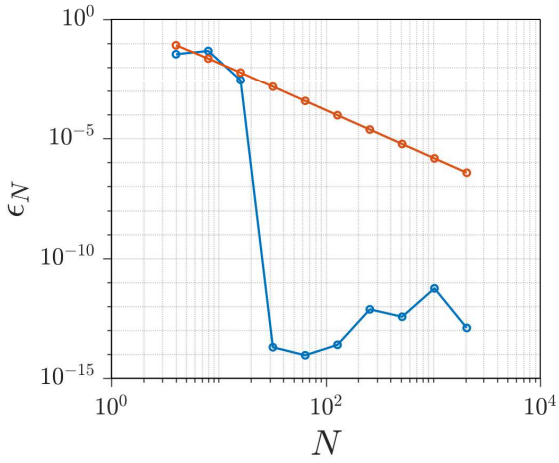

Figure 8: The convergence order of a spectral method and a finite difference method for the integration of $\ddot{x}(t) + x(t) = 0$.

Table 1: The convergence order of the FCC method and a finite difference method for integrating $\ddot{x}(t) + x(t) = 0$.

FCC method		Finite difference method	
N	$\mathcal{CO}$	h	$\mathcal{CO}$
4	0.46	0.2500	1.85
8	−4.08	0.1250	1.94
16	−37.11	0.0625	1.99
32	−1.12	0.0313	2.00
64	1.46	0.0156	2.00
128	4.92	0.0078	2.00
256	−1.03	0.0039	2.00
512	3.95	0.0020	2.00

Table 2: The convergence order of the solution in Example 6.2 by using the FCC and P(EC)$^{\mathrm{m}}$E method when $F_0 = 1.02$ and $\alpha = 0.8$.

FCC method			P(EC)$^{\mathrm{m}}$E method		
N	$\mathcal{CO}_i^{(I)}$	$\mathcal{CO}_i^{(II)}$	h	$\mathcal{CO}_i^{(I)}$	$\mathcal{CO}_i^{(II)}$
140	-9.16	-9.13	0.0071	1.10	1.04
196	-9.89	-9.85	0.0051	1.13	1.08
275	-18.67	-18.66	0.0036	1.15	1.11
385	-20.78	-23.22	0.0026	1.16	1.14
538	1.05	-3.97	0.0019	1.17	1.16
753	-0.24	7.32	0.0013	1.18	1.17

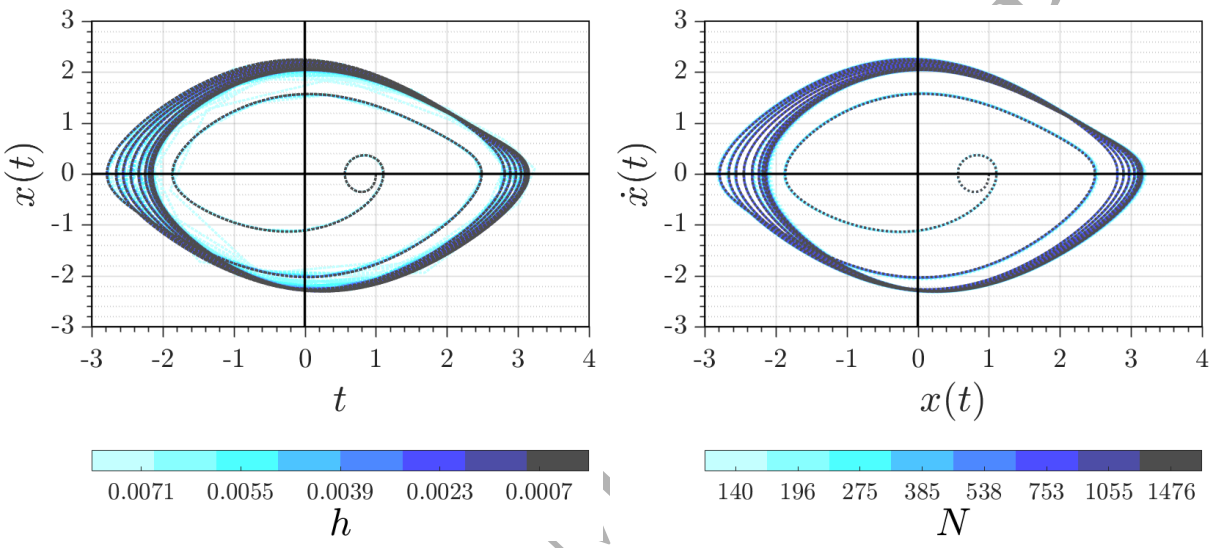

Figure 9: Numerical solution of Example 6.2 by using (a) the P(EC)$^{\mathrm{m}}$E method and (b) the FCC method.

We shall compare the performance of the FCC method with the P(EC)$^{\mathrm{m}}$E method of Adams-Bashforth-Moulton type described in [66]. Moreover, the number of multiple corrector iterations is chosen such as evaluated for a certain number of times until convergence of the iterations is reached [66]. The maximum number of iteration is set to $m = 100$ with the tolerance of $\varepsilon_m = 10^{-8}$. The solution obtained by the FCC method with $N = 1476$ is considered as the reference solution in the first criterion. The factor λ is 1.4 in the second criterion. For the FCC method, the nonlinear solver is the Newton-Raphson algorithm whose initial gauss is the solution obtained by using the P(EC)$^{\mathrm{m}}$E method with step size of $h = 0.01$.

The phase portrait of the system (98) via the FCC and P(EC)$^{\mathrm{m}}$E methods are illustrated in Fig. 9. Although the responses are indistinguishable by using the both methods, the FCC method has spectral convergence. Moreover, Table 2 shows the convergence order of the both methods calculated at the last collocation point in $t \in [0, 100]$. It shows that the FCC method performs significantly better than the P(EC)$^{\mathrm{m}}$E method where the convergence order of the FCC method is spectral in compare to that of the P(EC)$^{\mathrm{m}}$E method which is about 1.1. The convergence order of the FCC method decreases exponential by increasing N to achieve the approximation error in range of the machine precision (when $N \approx 385$). After that, the approximation error does not change significantly and fluctuates around zero for which those numbers of collocation points are shown in the red color cells of Table 2.

Example 6.3 (Fractional Hayes equation)**.** The FDE in Eq. (52) is named the fractional Hayes

Table 3: Numerical computation error by using the FCC and the Adams-Bashforth method for Example 6.3 when $\tau = 1$, $\phi(t) = 1$ and $t \in [0, 10]$.

FCC method			Adams-Bashforth Method		
N	$\varepsilon_N(\alpha = 1)$	$\varepsilon_N(\alpha = 1 - 10^{-14})$	h	$\varepsilon_N(\alpha = 1)$	$\varepsilon_N(\alpha = 1 - 10^{-14})$
100	1.19×10^{-13}	4.56×10^{-03}	0.0100	-4.39×10^{-05}	6.53×10^{-02}
200	1.43×10^{-13}	3.93×10^{-03}	0.0050	-1.09×10^{-05}	3.31×10^{-02}
300	3.34×10^{-13}	1.04×10^{-03}	0.0033	-4.84×10^{-06}	2.22×10^{-02}
400	8.51×10^{-13}	7.52×10^{-04}	0.0025	-2.72×10^{-06}	1.67×10^{-02}

equation which is the α-order scalar equation with a single point delay (see [12, 51]). Let the initial function $\phi(t) = 1$, $t \in [-\tau, 0]$ and $\tau = 1$. In the case $\alpha = 1$, the analytical solution can be expressed by a direct integration of $x(t)$ at the subsequence intervals $[(i-1), i]$, $i = 1, 2, \cdots$, i.e.

$$x(t) = \begin{cases} 1, & -1 \le t \le 0, \\ 1 - x, & 0 \le t \le 1, \\ \frac{1}{2}x^2 - 2x + \frac{3}{2}, & 1 \le t \le 2, \\ -\frac{x^3}{6} + \frac{3}{2}x^2 - 4x + \frac{17}{6}, & 2 \le t \le 3, \\ \vdots \end{cases} \tag{103}$$

Let the mean average error be defined as

$$\varepsilon_N = \frac{1}{N}\|e_n\|_1. \tag{104}$$

The solution can be obtained by a unique monodromy operator defined in Proposition 3.4. Table 3 shows the error obtained by the FCC method and that of the Adams-Bashforth method proposed in [67]. Since the monodromy matrix is a local operator in this case, the spectral convergence is expected shown in Table 3. On the other hand, let α be a number very close to 1 such as $\alpha = 1 - 10^{-14}$, and hence the solution must be obtained by using Proposition 3.3 that requires interpolations. Therefore, the numerical solution obtained by the FCC method should not have the spectral convergence property. However, Table 3 verifies that the error obtained by the FCC method is smaller than that obtained by the Adams-Bashforth method.

Example 6.4 (Fractional delayed damped Mathieu equation)**.** Consider the fractional delayed damped Mathieu equation with a single delay and a fractional-order derivative of the delayed state:

$$\ddot{x}(t) + (a + b\cos(\Omega t))\, x(t) + {}_0^C\mathcal{D}_t^{\alpha}[x(t)] = d\, {}_0^C\mathcal{D}_t^{\beta}[x(t-\tau)] \tag{105}$$

subject to the initial function $\phi(t) = \sin(t)$, $-\tau \le t \le 0$, where $\Omega = 2\,\mathrm{rad/s}$, $\tau = 1\,\mathrm{sec}$, and $\alpha, \beta \in [0, 1]$. In [51], it is shown that the solution of Eq. (105) is asymptotically stable when $a = 50$, $b = 5$, $c = 0$, and $d = 0.5$ for any initial function $\phi(t)$ and fractional order α. Let $a = 50$, $b = 5$, $c = 1$, and $d = 0.5$, then the space realization of Eq. (105) in the form of Eq. (41) is

$${}_0^C\mathcal{D}_t^{(1,1)}[\mathbf{x}(t)] = \begin{bmatrix} 0 & 1 \\ -(50 + 5\cos(\Omega t)) & 0 \end{bmatrix}\mathbf{x}(t) + \begin{bmatrix} 0 & 0 \\ 0 & -1 \end{bmatrix} {}_0^C\mathcal{D}_t^{(0,\alpha)}[\mathbf{x}(t)] + \begin{bmatrix} 0 & 0 \\ 0 & -0.5 \end{bmatrix} {}_0^C\mathcal{D}_t^{(0,\beta)}\mathbf{x}(t-\tau). \tag{106}$$

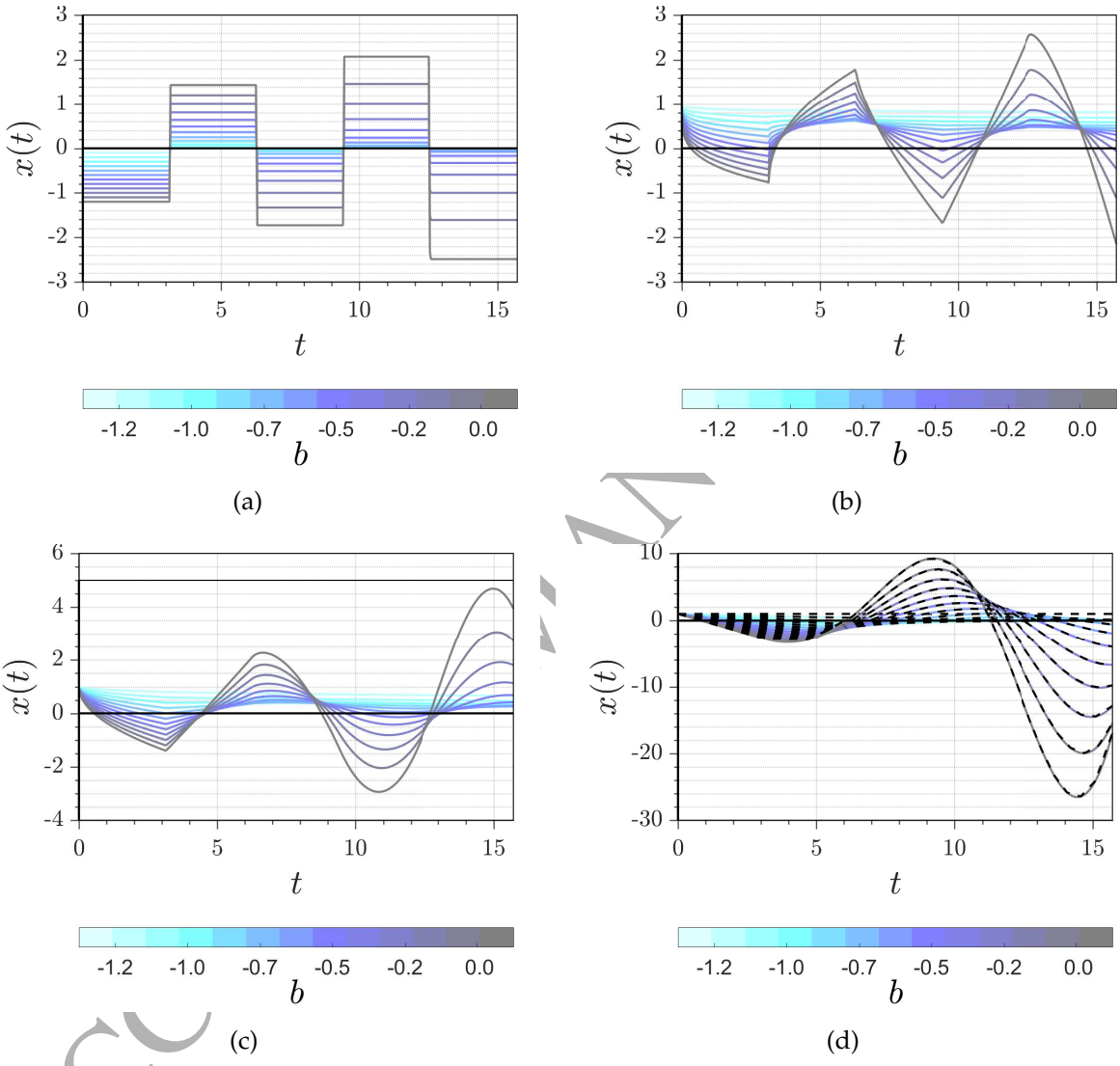

Figure 10: The numerical solution of Example 6.3 by using the FCC method for different values of b when $a = 0$, $\tau = \pi/2$, and (a) $\alpha = 0$, (b) $\alpha = 0.25$, (c) $\alpha = 0.5$, and (d) $\alpha = 1$ in which the dashed lines are the solution obtained by the `dde23`-solver in MATLAB.

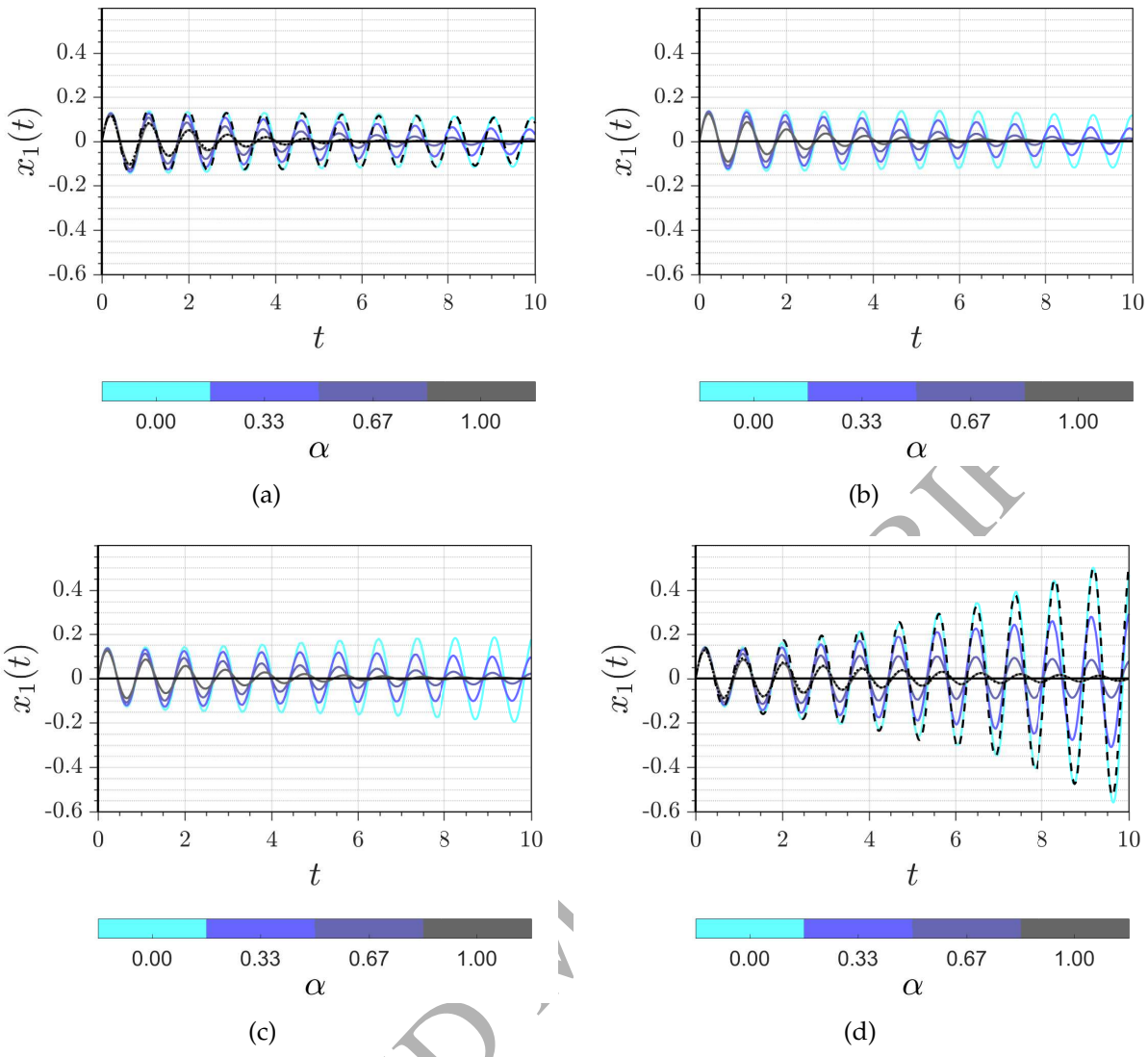

Figure 11: The numerical solution of Example 6.4 using the FCC method for different values of α: (a) $\beta = 0$, and dashed and dotted lines represent the integer-order solution when $\alpha = 0$ and $\alpha = 1$, respectively; (b) $\beta = 0.33$; (c) $\beta = 0.67$; (d) $\beta = 1$, and dashed and dotted lines represent the integer solution when $\alpha = 0$ and $\alpha = 1$, respectively.

It is noticed that the FDDE in Eq. (106) is not represented in commensurate order in general. Using 300 CGL collocation points results in discretizing $A(t)$ and $A_\alpha(t)$ as 600×600 matrices $\mathbf{A}_{d_t}$ and $\mathbf{A}_{\alpha_{d_t}}$. Figure 11 shows the numerical solutions for Eq. (105) obtained for different values of α and β using the FCC method. In the cases that α and β are integer (zero or one in this problem), then the `dde23` solver in MATLAB can be used to validate results as shown by the dashed and dotted lines in Figs. 11-(a) and -(d).

Example 6.5 (Irrational multiple delays)**.** Consider the following FDEs with multiple delays and a fractional-order derivative of the delayed coordinate:

$$\ddot{x}(t) + 5\dot{x}(t) + x(t) + 2x(t-\tau_1) + {}_0^C\mathcal{D}_t^\alpha\left[x(t-\tau_2)\right] - \pi x(t-\tau_3) = 0, \quad 0 \le \alpha \le 1, \tag{107}$$

with initial function $x(t) = \phi(t) = \sin(t)$, $-\tau_3 \le t \le 0$, where the delays are chosen as irrational numbers such as $\tau_1 = e/2$, $\tau_2 = e/\pi$, and $\tau_3 = \pi$. The state-space of Eq. (107) is realized as

$$\dot{\mathbf{x}}(t) = \begin{bmatrix} x_2(t) \\ -5x_2(t) - x_1(t) - 2x_1(t-\tau_1) - {}_0^C\mathcal{D}_t^\alpha\left[x_1(t-\tau_2)\right] + \pi x_1(t-\tau_3) \end{bmatrix}, \tag{108}$$

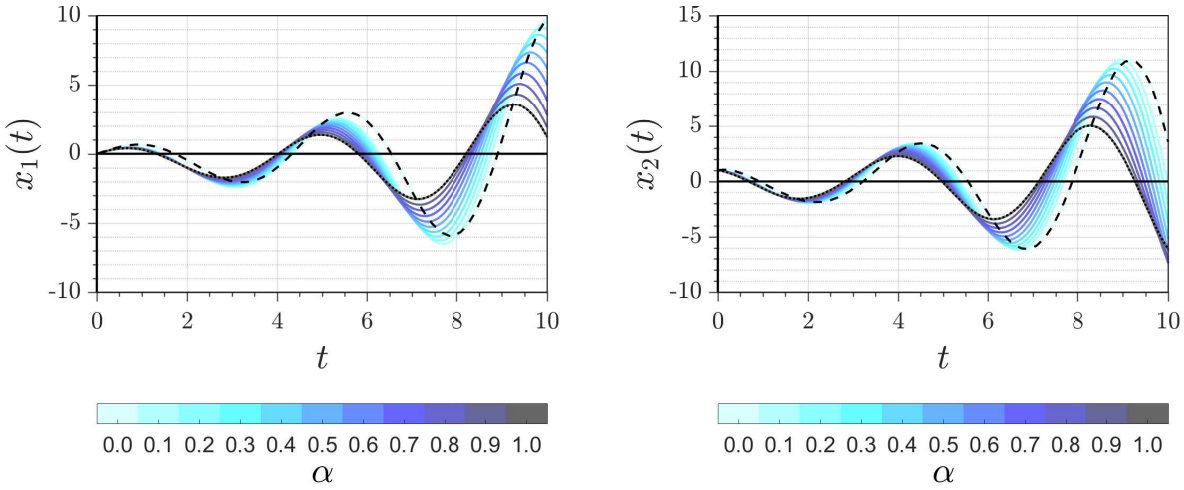

Figure 12: The numerical solution of Example 6.5 by using the FCC method for different values of α compared to the solution obtained by the`dde23`-solver in MATLAB when $\alpha = 0$ (dotted line) and $\alpha = 1$ (dashed line).

and hence the corresponding initial function becomes $\boldsymbol{\phi}(t) = [\sin(t),\ \cos(t)]^T$, $-\tau_3 \leq t \leq 0$. The solution of Eq. (107) is demonstrated in Fig. 12 for different values of α. Figure 12 shows that the solutions of the FCC method is similar to the ones obtained by `dde23` when $\alpha = 0$ or $\alpha = 1$.

7 Conclusions

In this paper, a framework was proposed for solving FDEs and FDDEs with multiple delays by spectral collocation methods. This framework can be used to obtain the numerical solution of a system of commensurate order FDEs or a system of linear FDDEs with multiple delays. The framework was enhanced with the FCC method based on discretizing the solution at the Chebyshev-Gauss-Lobatto points and defining a state-transition matrix for the interval of the solution. The FCC framework has superior advantages such as spectral convergence, small computational time, and noncanonical form representation with incommensurate orders. These advantages were illustrated in solving several numerical examples.

References

[1] J. T. Machado, "Fractional order description of dna," *Applied Mathematical Modelling*, vol. 39, no. 14, pp. 4095–4102, 2015.

[2] J. T. Machado and A. M. Lopes, "A fractional perspective on the trajectory control of redundant and hyper-redundant robot manipulators," *Applied Mathematical Modelling*, 2016.

[3] S. Kumar, "A new analytical modelling for fractional telegraph equation via laplace transform," *Applied Mathematical Modelling*, vol. 38, no. 13, pp. 3154–3163, 2014.

[4] R. Hilfer, *Applications of Fractional Calculus in Physics*. World Scientific, 2000.

[5] S. G. Samko, A. A. Kilbas, and O. I. Marichev, *Fractional Integrals and Derivatives: Theory and Applications*. Gordon & Breach Sci. Publishers, 1993.

[6] N. Heymans and J.-C. Bauwens, "Fractal rheological models and fractional differential equations for viscoelastic behavior," *Rheologica Acta*, vol. 33, no. 3, pp. 210–219, 1994.

[7] S. Das, *Functional Fractional Calculus*. Springer, 2011.

[8] R. L. Bagley and P. J. Torvik, "On the fractional calculus model of viscoelastic behavior," *Journal of Rheology (1978-Present)*, vol. 30, no. 1, pp. 133–155, 1986.

[9] G. Stepan, "Delay effects in the human sensory system during balancing," *Philosophical Transactions of The Royal Society of London A: Mathematical, Physical and Engineering Sciences*, vol. 367, no. 1891, pp. 1195–1212, 2009.

[10] Y. Boukal, M. Zasadzinski, M. Darouach, and N.-E. Radhy, "Robust functional observer design for uncertain fractional-order time-varying delay systems," in *American Control Conference, ACC'2016*, 2016.

[11] Z. Wang, X. Huang, and J. Zhou, "A numerical method for delayed fractional-order differential equations: based on gl definition," *Applied Mathematics & Information Sciences*, vol. 7, no. 2L, pp. 525–529, 2013.

[12] E. A. Butcher, A. Dabiri, and M. Nazari, "Transition Curve Analysis of Linear Fractional Periodic Time-Delayed Systems via Explicit Harmonic Balance Method," *Journal of Computational and Nonlinear Dynamics*, vol. 11, no. 4, p. 041005, 2016.

[13] L. N. Trefethen, *Spectral Methods in MATLAB*, vol. 10. Siam, 2000.

[14] J. P. Boyd, *Chebyshev and Fourier Spectral Methods*. Courier Corporation, 2001.

[15] K. Diethelm, N. J. Ford, and A. D. Freed, "A predictor-corrector approach for the numerical solution of fractional differential equations," *Nonlinear Dynamics*, vol. 29, no. 1-4, pp. 3–22, 2002.

[16] B. Moghaddam and J. Machado, "A stable three-level explicit spline finite difference scheme for a class of nonlinear time variable order fractional partial differential equations," *Computers & Mathematics with Applications*, 2016.

[17] D. Baleanu, K. Diethelm, E. Scalas, and J. J. Trujillo, *Fractional calculus: models and numerical methods*, vol. 5. World Scientific, 2016.

[18] X. Ma and C. Huang, "Spectral collocation method for linear fractional integro-differential equations," *Applied Mathematical Modelling*, vol. 38, no. 4, pp. 1434–1448, 2014.

[19] I. Ameen and P. Novati, "The solution of fractional order epidemic model by implicit adams methods," *Applied Mathematical Modelling*, vol. 43, pp. 78–84, 2017.

[20] F. Liu, P. Zhuang, I. Turner, K. Burrage, and V. Anh, "A new fractional finite volume method for solving the fractional diffusion equation," *Applied Mathematical Modelling*, vol. 38, no. 15, pp. 3871–3878, 2014.

[21] H. Ding and C. Li, "Fractional-compact numerical algorithms for Riesz spatial fractional reaction-dispersion equations," *Fractional Calculus and Applied Analysis*, vol. 20, no. 3, pp. 722–764, 2017.

[22] H. Ding and C. Li, "High-order algorithms for Riesz derivative and their applications (iii)," *Fractional Calculus and Applied Analysis*, vol. 19, no. 1, pp. 19–55, 2016.

[23] H. Ding, C. Li, and Y. Chen, "High-order algorithms for Riesz derivative and their applications (ii)," *Journal of Computational Physics*, vol. 293, pp. 218–237, 2015.

[24] C. Li and F. Zeng, *Numerical methods for fractional calculus*, vol. 24. CRC Press, 2015.

[25] B. P. Moghaddam and J. A. T. Machado, "A computational approach for the solution of a class of variable-order fractional integro-differential equations with weakly singular kernels," *Fractional Calculus and Applied Analysis*, vol. 20, no. 4, pp. 1023–1042, 2017.

[26] B. Moghaddam, J. Machado, and H. Behforooz, "An integro quadratic spline approach for a class of variable-order fractional initial value problems," *Chaos, Solitons & Fractals*, 2017.

[27] S. Yaghoobi, B. P. Moghaddam, and K. Ivaz, "An efficient cubic spline approximation for variable-order fractional differential equations with time delay," *Nonlinear Dynamics*, vol. 87, no. 2, pp. 815–826, 2017.

[28] A. Dabiri and E. A. Butcher, "Efficient modified Chebyshev differentiation matrices for fractional differential equations," *Communications in Nonlinear Science and Numerical Simulation*, vol. 50, no. ISSN 1007-5704, pp. 584–310, 2017.

[29] A. Dabiri and E. A. Butcher, "Stable fractional Chebyshev differentiation matrix for numerical solution of fractional differential equations," *Nonlinear Dynamics*, vol. 90, no. 1, pp. 185–201, 2017.

[30] P. Mokhtary, F. Ghoreishi, and H. Srivastava, "The müntz-Legendre Tau method for fractional differential equations," *Applied Mathematical Modelling*, vol. 40, no. 2, pp. 671–684, 2016.

[31] E. Keshavarz, Y. Ordokhani, and M. Razzaghi, "Bernoulli wavelet operational matrix of fractional order integration and its applications in solving the fractional order differential equations," *Applied Mathematical Modelling*, vol. 38, no. 24, pp. 6038–6051, 2014.

[32] A. Bhrawy and M. Zaky, "Shifted fractional-order jacobi orthogonal functions: application to a system of fractional differential equations," *Applied Mathematical Modelling*, vol. 40, no. 2, pp. 832–845, 2016.

[33] A. Saadatmandi, "Bernstein operational matrix of fractional derivatives and its applications," *Applied Mathematical Modelling*, vol. 38, no. 4, pp. 1365–1372, 2014.

[34] C. Li, Q. Yi, and A. Chen, "Finite difference methods with non-uniform meshes for nonlinear fractional differential equations," *Journal of Computational Physics*, vol. 316, pp. 614–631, 2016.

[35] C. Li and F. Zeng, "The finite difference methods for fractional ordinary differential equations," *Numerical Functional Analysis and Optimization*, vol. 34, no. 2, pp. 149–179, 2013.

[36] C. Hwang and Y.-C. Cheng, "A numerical algorithm for stability testing of fractional delay systems," *Automatica*, vol. 42, no. 5, pp. 825–831, 2006.

[37] M. Busłowicz, "Stability of linear continuous-time fractional order systems with delays of the retarded type," *BULLETIN OF THE POLISH ACADEMY OF SCIENCES TECHNICAL SCIENCES*, vol. 56, no. 4, 2008.

[38] M. L. Morgado, N. J. Ford, and P. Lima, "Analysis and numerical methods for fractional differential equations with delay," *Journal of Computational and Applied Mathematics*, vol. 252, pp. 159–168, 2013.

[39] S. Bhalekar and V. Daftardar-Gejji, "A predictor-corrector scheme for solving nonlinear delay differential equations of fractional order," *Journal of Fractional Calculus and Applications*, vol. 1, no. 5, pp. 1–9, 2011.

[40] B. P. Moghaddam, S. Yaghoobi, and J. T. Machado, "An extended predictor-corrector algorithm for variable-order fractional delay differential equations," *Journal of Computational and Nonlinear Dynamics*, 2016.

[41] U. Saeed *et al.*, "Hermite wavelet method for fractional delay differential equations," *Journal of Difference Equations*, vol. 2014, 2014.

[42] M. Zheng, F. Liu, V. Anh, and I. Turner, "A high-order spectral method for the multiterm time-fractional diffusion equations," *Applied Mathematical Modelling*, vol. 40, no. 7, pp. 4970–4985, 2016.

[43] P. Mokhtary and F. Ghoreishi, "The l 2-convergence of the Legendre spectral tau matrix formulation for nonlinear fractional integro differential equations," *Numerical Algorithms*, vol. 58, no. 4, pp. 475–496, 2011.

[44] K. Maleknejad, K. Nouri, and L. Torkzadeh, "Operational matrix of fractional integration based on the shifted second kind Chebyshev polynomials for solving fractional differential equations," *Mediterranean Journal of Mathematics*, vol. 13, no. 3, pp. 1377–1390, 2016.

[45] F. Ghoreishi and S. Yazdani, "An extension of the spectral Tau method for numerical solution of multi-order fractional differential equations with convergence analysis," *Computers & Mathematics with Applications*, vol. 61, no. 1, pp. 30–43, 2011.

[46] Z. Li, L. Liu, S. Dehghan, Y. Chen, and D. Xue, "A review and evaluation of numerical tools for fractional calculus and fractional order controls," *International Journal of Control*, pp. 1–17, 2016.

[47] I. Podlubny, I. Petráš, T. Skovranek, and J. Terpák, "Toolboxes and programs for fractional-order system identification, modeling, simulation, and control," in *Carpathian Control Conference (ICCC), 2016 17th International*, pp. 608–612, IEEE, 2016.

[48] A. Tepljakov, E. Petlenkov, and J. Belikov, "FOMCON: a MATLAB toolbox for fractional-order system identification and control," *International Journal of Microelectronics and Computer Science*, vol. 2, no. 2, pp. 51–62, 2011.

[49] Y. Chen, I. Petras, and D. Xue, "Fractional order control-a tutorial," in *American Control Conference, 2009. ACC'09.*, pp. 1397–1411, IEEE, 2009.

[50] A. Dabiri, "Guide to FCC: Stability and solution of linear time variant fractional differential equations with spectral convergence using the FCC toolbox package in MATLAB." http://u.arizona.edu/~armandabiri/fcc.html, 2017. [Online; accessed 26-July-2017].

[51] E. A. Butcher, A. Dabiri, and M. Nazari, "Stability and Control of Fractional Periodic Time-delayed Systems," in *Time Delay Systems: Theory, Numerics, Applications, and Experiments* (T. Insperger, T. Ersal, and G. Orosz, eds.), vol. 7, pp. 107–125, Springer, New York, 2017.

[52] L. F. Shampine and S. Thompson, "Solving ddes in matlab," *Applied Numerical Mathematics*, vol. 37, no. 4, pp. 441–458, 2001.

[53] A. A. Kilbas, H. M. Srivastava, and J. J. Trujillo, *Theory and Applications of Fractional Differential Equations*, vol. 204. New York, NY: Elsevier Science Inc., 2006.

[54] M. Caputo and F. Mainardi, "A new dissipation model based on memory mechanism," *Pure and Applied Geophysics*, vol. 91, no. 1, pp. 134–147, 1971.

[55] A. Dabiri, E. A. Butcher, and M. Nazari, "Coefficient of restitution in fractional viscoelastic compliant impacts using fractional Chebyshev collocation," *Journal of Sound and Vibration*, vol. 388, pp. 230–244, 2017.

[56] G. Herrmann, "Stability of equilibrium of elastic systems subjected to nonconservative forces(stability of equilibrium of elastic systems under nonconservative load, discussing criteria of stability, modes of instability, follower force problems, etc)," *Applied Mechanics Reviews*, vol. 20, pp. 103–108, 1967.

[57] A. Bogdanov, "Optimal control of a double inverted pendulum on a cart," *Oregon Health and Science University, Tech. Rep. CSE-04-006, OGI School of Science and Engineering, Beaverton, OR*, 2004.

[58] M. Tavakoli-Kakhki and M. Haeri, "The minimal state space realization for a class of fractional order transfer functions," *SIAM Journal on Control and Optimization*, vol. 48, no. 7, pp. 4317–4326, 2010.

[59] M. Tavakoli-Kakhki, M. Haeri, and M. S. Tavazoei, "Notes on the state space realizations of rational order transfer functions," *IEEE Transactions on Circuits and Systems I: Regular Papers*, vol. 58, no. 5, pp. 1099–1108, 2011.

[60] M. S. Tavazoei and M. Tavakoli-Kakhki, "Minimal realizations for some classes of fractional order transfer functions," *IEEE Journal on Emerging and Selected Topics in Circuits and Systems*, vol. 3, no. 3, pp. 313–321, 2013.

[61] A. Dabiri, E. A. Butcher, M. Poursina, and M. Nazari, "Optimal periodic-gain fractional delayed state feedback control for linear fractional periodic time-delayed systems," *IEEE Transactions on Automatic Control*, 2017, Date of Publication: 24 July 2017.

[62] D. Matignon, "Stability results for fractional differential equations with applications to control processing," in *Computational engineering in systems applications*, vol. 2, pp. 963–968, IMACS, IEEE-SMC Lille, France, 1996.

[63] C. Canuto, M. Hussaini, A. Quarteroni, and T. Zang, *Spectral Methods: Fundamentals in Single Domains*. Springer-Verlag Berlin Heidelberg, 2007.

[64] C. De Boor, C. De Boor, E.-U. Mathématicien, C. De Boor, and C. De Boor, *A practical guide to splines*, vol. 27. Springer-Verlag New York, 1978.

[65] A. Dabiri, M. Nazari, and E. A. Butcher, "Chaos analysis and control in fractional-order systems using fractional Chebyshev collocation method," in *ASME 2016 International Mechanical Engineering Congress & Exposition (IMECE)*, Phoenix, AZ, Nov 11–17, 2016.

[66] K. Diethelm and A. D. Freed, "The FracPECE subroutine for the numerical solution of differential equations of fractional order," *Forschung und wissenschaftliches Rechnen*, vol. 1999, pp. 57–71, 1998.

[67] K. Diethelm, "An algorithm for the numerical solution of differential equations of fractional order," *Electronic transactions on numerical analysis*, vol. 5, no. 1, pp. 1–6, 1997.